Computational Economics
https://doi.org/10.1007/s10614-026-11390-z

On Discontinuity and Persistence in the Returns on Financial Assets: New Simulation-Based Evidence Derived From a Multifractal Model of Asset Returns

Klaus Grobys[1,2]

Received: 20 December 2025 / Accepted: 29 June 2026

Abstract

According to Mandelbrot, financial assets are characterized by two characteristic traits—discontinuity and price persistence. This paper uses simulations to obtain predictions for these two key features derived from a multifractal model of asset returns (MMAR). Following Mandelbrot, this paper uses the exponents of power laws to study asset return discontinuity, whereas the level of price persistence is measured via Hurst exponents. Using the distributions of these exponents derived from MMAR simulations, this study proposes a novel joint test designed to examine whether the MMAR is capable of describing the return data on financial assets with respect to these two key traits. Intriguingly, empirical tests suggest that the benchmark MMAR specification employed here is capable of describing discontinuity and persistence observed for the returns on five key financial asset markets—U.S. equities, USD/GBP exchange rates, gold futures, crude oil futures and Bitcoin. From a theoretical perspective, the findings are consistent with the possibility that common latent mechanisms, including herding behavior, may contribute to return dynamics across otherwise unrelated asset markets.

Keywords Bitcoin · Cryptocurrency · Price persistence · Hurst exponent · Multifractality · Power laws

JEL Classification C14 · C22 · C60 · G10 · G17

✉ Klaus Grobys
klaus.grobys@uwasa.fi

1 Finance and Financial Accounting Research Group, School of Accounting and Finance, University of Vaasa, Wolffintie 34, 65200 Vaasa, Finland

2 Innovation and Entrepreneurship (InnoLab), University of Vaasa, Wolffintie 34, 65200 Vaasa, Finland

Published online: 15 July 2026

1 Introduction

Mandelbrot et al. (1997) were the first to propose a multifractal model of asset returns (MMAR), a model designed to generate time-series evolutions resembling asset returns. Mandelbrot (2008) emphasized that financial asset prices exhibit two key features: discontinuity and price persistence. In his account, markets are described as “deforming time,” in the sense that time is either expanded or contracted, and the more severe these changes are, the more trading time expands. At the same time, Mandelbrot (2008) stressed that this notion of time deformation should be understood primarily as a mathematical convenience for analyzing financial returns rather than as a literal proxy for trading volume. In the original MMAR of Mandelbrot et al. (1997), time deformation is generated by binominal bending that is iterated to form a multiplicative cascade, which constitutes the essential building block of the model. A single multiplicative cascade can therefore generate infinitely many time-series evolutions with statistical properties resembling those of financial asset returns. Hence, in this study, ‘time deformation’ or ‘trading time’ is understood as a latent model-based time scale that may expand or contract relative to calendar time, thereby reflecting variation in the intensity of market activity in the return-generating process.

The seminal contribution of Mandelbrot et al. (1997) stimulated a broader literature on alternative multiplicative cascades and related multifractal specifications of asset returns. For example, Calvet and Fisher (2002) studied time deformations derived from Poisson and gamma distributions. Other multifractal constructions have been developed by Muzy and Bacry (2002), Bacry et al. (2008), Calvet et al. (2018), and Lux et al. (2014), while Segnon and Lux (2013) provide an extensive overview of this literature. More recent literature has also applied fractal and multifractal methods to cryptocurrency markets. For instance, Stavroyiannis et al. (2019) study the fractal dynamics of Bitcoin using wavelet modulus maxima and detrended fluctuation analysis, while Gradojevic and Tsiakas (2021) examine volatility dynamics in cryptocurrencies using multiplicative cascades. More recent evidence by Takaishi (2025) further suggests that Bitcoin volatility exhibits multifractal features and time-scale-dependent persistence.

Acknowledging Mandelbrot’s (2008) view that financial assets are characterized by discontinuity and price persistence, the purpose of this study is to provide simulation-based evidence on MMAR predictions for these two key traits of financial asset returns. Following Mandelbrot (2008), discontinuity is examined through power-law behavior, whereas persistence is evaluated through the Hurst exponent. The analysis focuses on whether the MMAR can jointly account for both features and whether this ability depends on the degree of time deformation embedded in the multiplicative cascade.

This study contributes to the literature in three closely related ways. First, it complements Calvet and Fisher (2002), who examined multifractality in moment scaling, by shifting attention to two core implications of the MMAR emphasized by Mandelbrot (2008): power-law behavior associated with discontinuity and long-range persistence in returns. Second, the study develops a joint test designed to assess whether the MMAR can simultaneously account for these two characteristic features of financial asset returns. Third, the analysis extends the benchmark MMAR by considering multiplicative cascades that imply milder or wilder time deformation than in the original formulation, thereby allowing a systematic comparison of how alternative cascade structures shape the model's predictions.

The paper is also related to the literature on power laws and tail risk in financial economics. Several studies suggest that tail risk may vary over time (Galbraith & Zernov, 2004; Quintos et al., 2001; Wagner, 2003; Werner & Upper, 2004). Motivated by this literature, Kelly (2014) and Kelly and Jiang (2014) developed a dynamic tail-risk measure based on a panel approach and showed that the resulting tail exponent is highly persistent. By contrast, Grobys (2024) reported strong evidence of total invariance in the power-law behavior of realized foreign exchange rate variances across time and frequencies. Against this background, the present study examines whether MMAR-based predictions are more consistent with invariance or with time-dependence in the power-law behavior of financial returns., This issue matters because time-varying tail risk would imply that the magnitudes of extreme events are not governed by a common underlying functional law, whereas Mandelbrot (2008) argued that invariances in data-generating processes are particularly valuable because they improve the reliability of inference and prediction.

In addition to traditional financial markets, the analysis includes Bitcoin as a proxy for the cryptocurrency market. This extension is relevant because cryptocurrencies are widely associated with recurrent extreme events and unusually high volatility (Baur & Dimpfl, 2021; Kyriazis et al., 2020). Recent work such as Liu et al.'s (2022) three-factor model approaches cryptocurrency returns from the perspective of conventional asset pricing, in the spirit of Fama and French (1992, 1993, 2015). The present study instead takes a fractal perspective and asks whether the benchmark MMAR specification employed here can also account for the discontinuity and persistence observed in Bitcoin returns. In this sense, the paper extends MMAR-based evidence to a market that differs markedly from traditional asset classes yet is often characterized by pronounced nonlinear dynamics.

Overall, the findings show that the benchmark MMAR and its extensions generate empirically meaningful predictions for discontinuity and persistence, and that the original specification performs remarkably well across the financial assets considered, including Bitcoin. More broadly, the results are consistent with the view that similar underlying mechanisms may govern return dynamics across otherwise very different asset markets. Since power-law behavior in financial returns is often interpreted as a manifestation of herding behavior (Lux, 1995; Lux & Marchesi, 1999), the evidence is consistent with the view that common latent mechanisms may underlie discontinuity and persistence across traditional and cryptocurrency markets alike.

The remainder of the paper is organized as follows. Section 2 describes the data. Section 3 introduces the methodology. Section 4 presents the results. Section 5 discusses the findings, and Section 6 concludes.

2 Data for the Statistical Tests on Empirical Data

For the empirical part of this study, weekly log-return data on the U.S. S&P 500, USD/GBP exchange rate, gold futures (Dec 24 (GCZ4)), crude oil futures (Nov 24 (CLX4)), and Bitcoin were downloaded from investing.com. The return series are aligned on a common weekly sample period from January 3, 2016 to September 22, 2024, yielding 456 weekly observations for each asset. The common sample period is determined by data availability for Bitcoin. No additional data filtering or outlier adjustment is applied.

In addition, monthly log-return data on the U.S. S&P 500, USD/GBP exchange rate, gold, and crude oil were obtained from stooq.com and used for a robustness analysis. The monthly sample runs from October 1981 to March 2026, yielding 534 monthly observations for each asset. The starting date of the monthly sample is determined by data availability for crude oil in the database, as observations prior to October 1981 contain consecutive months with zero log returns and were excluded from the analysis. No additional data filtering or outlier adjustment is applied to the monthly series.

Descriptive statistics are reported in Table 11 in the Appendix. As shown there, the weekly return series (Panel A) exhibit pronounced non-normality and excess kurtosis. In particular, kurtosis ranges from 5.023 for Bitcoin to 9.67 for the S&P 500, which points to substantially heavier tails than under a normal distribution. Consistent with this observation, the Jarque–Bera test rejects normality for all weekly assets at conventional significance levels. The monthly return series (Panel B) also exhibit substantial departures from normality, with kurtosis ranging from 4.24 for gold to 12.37 for crude oil, and the Jarque–Bera test again rejecting normality for all assets. These distributional features support the relevance of modeling discontinuity through power-law behavior in the return-generating process.

3 Methodology

3.1 Generating Multifractal Asset Return Data by Means of the MMAR

In their highly influential, yet surprisingly unpublished 1997 paper, Mandelbrot and his collaborators were the first to propose the MMAR designed to mimic the returns on financial assets. Whereas Mandelbrot et al.'s (1997) MMAR model incorporates the fractional Brownian motion to produce long-memories in asset returns while allowing for the possibility that financial asset returns themselves are independent, Mandelbrot (2008) suggested a simplified version of the MMAR that uses a plain normal distribution as opposed to a fractional Brownian motion. Mandelbrot et al. (1997) argued that, depending on the multiplicative cascade, a wide spectrum of tail behavior can be generated ranging from "mild" to "wild." Interestingly, in a recent paper, Grobys (2023) extended Mandelbrot et al. (1997) and Mandelbrot (2008) by proposing the multifractal model of asset invariances (MMAI) designed to model the second moment of financial assets. Grobys (2023) showed that the higher the level of time deformation is chosen, the more extreme is the tail behavior and the higher is the level of variance persistence. Consequently, the evidence derived from Grobys' (2023) study suggests that long-range dependence is not necessarily induced only by some fractional Brownian motion. Hence, extending Grobys' (2023) study, we investigate the impact of the level of time deformation on the predicted tail behavior (viz., power-law behavior) and persistence in the returns on financial assets as opposed to the realized second moment (viz., realized variance) of financial assets.

Following Mandelbrot (2008), the daily financial asset return process x_t of some financial asset is modeled as the product:

$$x_t = z_t \varepsilon_t, \tag{1}$$

where z_t denotes the multiplicative cascade component governing the latent scale variation in the return-generating process, and ε_t denotes a distribution that is assumed to be normal, $\varepsilon_t \sim IIDN(0,1)$. In the present implementation, the cascade-generated component z_t is used directly as the latent scale factor applied to the Gaussian innovation. In line with Mandelbrot et al. (1997) and Mandelbrot (2008), we use binominal bending to compute various multiplicative cascades. Specifically, the following probabilities, p, are employed to produce "deformed clock time" corresponding to "trading time:"

$$j = 1 : p = 0.55, \tag{1.1}$$

$$j = 2 : p = 0.60, \tag{1.2}$$

$$j = 3 : p = 0.65, \tag{1.3}$$

$$j = 4 : p = 0.70, \tag{1.4}$$

$$j = 5 : p = 0.75, \tag{1.5}$$

$$j = 6 : p = 0.80, \tag{1.6}$$

$$j = 7 : p = 0.85. \tag{1.7}$$

That is, we explore $j = 1, \ldots 7$ multiplicative cascades. Intuitively, a higher value of p implies a more uneven binomial branching of trading time and therefore a more concentrated multiplicative cascade. This produces stronger time deformation, which in turn is expected to generate wilder return dynamics, reflected in lower power-law exponents. Conversely, lower values of p imply milder time deformation and therefore less extreme tail behavior.

Following Grobys (2023), for each given multiplicative cascade j, this study uses $k = 13$ iterations, giving us $2^k = 2^{13} = 8{,}192$ daily observations for vector $\boldsymbol{z}_j$. Following the dyadic branching structure of the MMAR, the simulated series length is chosen as a power of two. Specifically, using $k = 13$ iterations yields $2^{13} = 8{,}192$ daily observations, which is consistent with the binomial cascade construction and with the simulation design commonly used in the multifractal literature (see, e.g., Grobys, 2023; Segnon & Lux, 2013). This choice also ensures that, after temporal aggregation, the simulated data provide sufficiently long weekly and monthly return series for the estimation of power-law and Hurst exponents and for comparison with the empirical analysis.

Next, the first 5,120 observations of vector $\boldsymbol{z}_j$ are employed to construct $b = 1, \ldots, B$ 5,120 × 1 vectors of multifractal asset returns by multiplying the elements $z_{1,j}$, $z_{2,j}$,…,$z_{5120,j}$ of the vector $\boldsymbol{z}_j$ array-by-array with random drawings from the standard normal distribution, $\varepsilon_{1,b}$, $\varepsilon_{2,b}$,…,$\varepsilon_{5120,b}$, resulting in $B = 1{,}000$ vectors, $\boldsymbol{x}_{bj}$, that is:

$$[\boldsymbol{x}_{1,j}\boldsymbol{x}_{2,j}\boldsymbol{x}_{3,j}\ldots\boldsymbol{x}_{B,j}] = \left[\begin{pmatrix} z_{1j}\varepsilon_{1,1} \\ z_{2j}\varepsilon_{2,1} \\ \vdots \\ z_{5120j}\varepsilon_{5120,1} \end{pmatrix} \begin{pmatrix} z_{1j}\varepsilon_{1,2} \\ z_{2j}\varepsilon_{2,2} \\ \vdots \\ z_{5120j}\varepsilon_{5120,2} \end{pmatrix} \begin{pmatrix} z_{1j}\varepsilon_{1,3} \\ z_{2j}\varepsilon_{2,3} \\ \vdots \\ z_{5120j}\varepsilon_{5120,3} \end{pmatrix} \cdots \begin{pmatrix} z_{1j}\varepsilon_{1,1000} \\ z_{2j}\varepsilon_{2,1000} \\ \vdots \\ z_{5120j}\varepsilon_{5120,1000} \end{pmatrix}\right].$$

Note again that all vectors $\boldsymbol{x}_{1,j}$, $\boldsymbol{x}_{2,j}$,…,$\boldsymbol{x}_{B,j}$ have the dimension 5,120 × 1 and use the same multiplicative cascade j, denoted as, $\boldsymbol{z}_j$, which, in turn, depends on p. Then, for $b = 1, \ldots, B$, weekly asset return vectors $\boldsymbol{x}_{b,j}^W$ are computed as:

$$\boldsymbol{x}_{b,j}^W = \left(\sum\nolimits_{t=1}^{5} x_{t,b,j}, \sum\nolimits_{t=6}^{10} x_{t,b,j}, \ldots, \sum\nolimits_{t=5116}^{5120} x_{t,b,j}\right)', \tag{2}$$

where $\boldsymbol{x}_{b,j}^M$ has the dimension 1,024 × 1. Furthermore, for $b = 1, \ldots, B$, monthly asset returns are calculated accordingly as:

$$\boldsymbol{x}_{b,j}^M = \left(\sum\nolimits_{t=1}^{20} x_{t,b,j}, \sum\nolimits_{t=21}^{40} x_{t,b,j}, \ldots, \sum\nolimits_{t=5101}^{5120} x_{t,b,j}\right)', \tag{3}$$

where $\boldsymbol{x}_{b,j}^M$ has the dimension 256 × 1. The simulation procedure is summarized in an illustrative manner in Fig. 1.

3.2 Predicted Discontinuity Derived From MMAR Simulations

Simulated financial asset returns are explored with respect to their two characteristic traits as identified by Mandelbrot (2008). Mandelbrot (2008) documented that the first characteristic trait that the returns on financial assets typically exhibit is *abrupt change* or *discontinuity*. A typical manifestation of this trait is the presence of a Paretian tail; specifically, the tail of financial asset returns is governed by some power-law process, measured by the characteristic power-law exponent. As pointed out in Lux and Alfarano (2016), power-law behavior is a "universal feature of financial assets." Therefore, to investigate the power-law behavior of financial asset return data generated by a given multiplicative cascade j, each vector $\boldsymbol{x}_{b,j}^W$ and $\boldsymbol{x}_{b,j}^M$ is modeled as a power law using the following model:

$$p\,(y) = By^{-\alpha}, \tag{4}$$

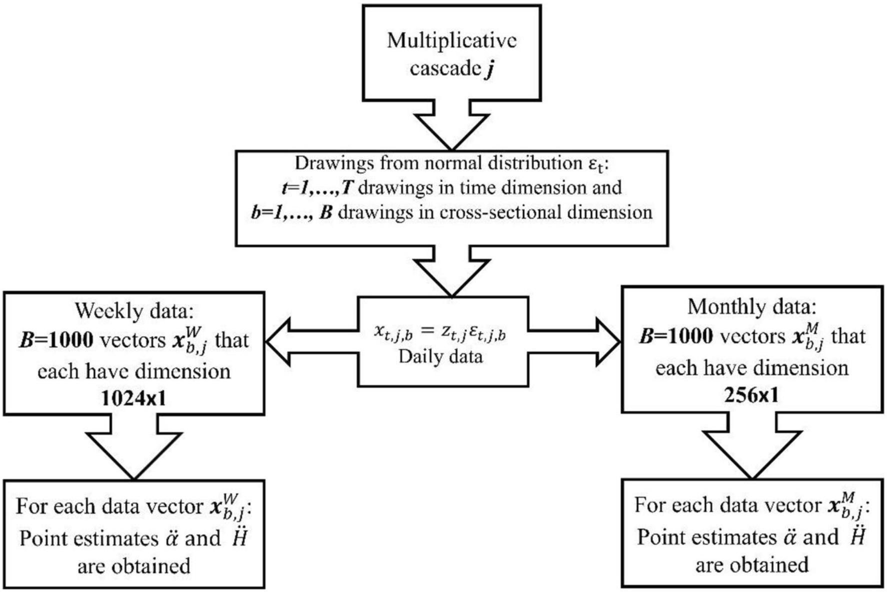

Fig. 1 Simulation procedure. This figure visualizes the simulation procedure to retrieve weekly and monthly asset return data by means of the multifractal model of asset returns. Following Mandelbrot (2008), the daily financial asset return process x_t of a financial asset is modeled as the product: $x_t = z_t\varepsilon_t$, where z_t denotes the multiplicative cascade serving as multifractal time, and ε_t denotes a distribution that is assumed to be normal, $\varepsilon_t \sim IIDN(0,1)$. In line with Mandelbrot et al. (1997) and Mandelbrot (2008), we use binominal bending of clock time to compute various multiplicative cascades. Specifically, the main analysis of this study uses the following probabilities to produce deformed clock time, respectively, trading time: $p = 0.55$ (e.g., $j = 1$), $p = 0.60$ (e.g., $j = 2$), $p = 0.65$ (e.g., $j = 3$), $p = 0.70$ (e.g., $j = 4$), $p = 0.75$ (e.g., $j = 5$),$p = 0.80$ (e.g., $j = 6$), $p = 0.85$ (e.g., $j = 7$). Following Grobys (2023), for each given multiplicative cascade j, this study uses $k = 13$ iterations, giving us $2^{13} = 8192$ daily observations for vector $\boldsymbol{z}_j$. The first 5120 observations of vector $\boldsymbol{z}_j$ are employed to construct $b = 1, \ldots, B$ 5120×1 vectors of multifractal asset returns by multiplying elements $z_{1,j}$, $z_{2,j}$,...,$z_{5120,j}$ with random drawings from the standard normal distribution, $\varepsilon_{1,b}$, $\varepsilon_{2,b}$,...,$\varepsilon_{5120,b}$, resulting in $B = 1000$ vectors for $\boldsymbol{x}$, that is: $\left[\boldsymbol{x}_{1,j}\boldsymbol{x}_{2,j}\boldsymbol{x}_{3,j}\ldots\boldsymbol{x}_{B,j}\right]$. All vectors $\boldsymbol{x}_{1,j}$, $\boldsymbol{x}_{2,j}$,...,$\boldsymbol{x}_{B,j}$ have the dimension 5120×1 and use the same multiplicative cascade $\boldsymbol{z}_j$ which, in turn, depends on p and $(1-p)$. Following Grobys (2023a), for $b = 1, \ldots, B$, weekly asset return vectors $\boldsymbol{x}^W_{b,j}$ are computed as, $\boldsymbol{x}^W_{b,j} = \left(\sum_{t=1}^{5} x_{t,b,j}, \sum_{t=6}^{10} x_{t,b,j}, \ldots, \sum_{t=5116}^{5120} x_{t,b,j}\right)'$, where $\boldsymbol{x}^M_{b,j}$ has the dimension 1024×1. Furthermore, for $b = 1, \ldots, B$, monthly asset returns are calculated accordingly as, $\boldsymbol{x}^M_{b,j} = \left(\sum_{t=1}^{20} x_{t,b,j}, \sum_{t=21}^{40} x_{t,b,j}, \ldots, \sum_{t=5101}^{5120} x_{t,b,j}\right)'$, where $\boldsymbol{x}^M_{b,j}$ has the dimension 256×1

where $y = |x|$, $B = (\alpha - 1)\, y_{MIN}^{\alpha-1}$ with $\alpha \in \{\mathbb{R}_+ | \alpha > 1\}$, $y \in \{\mathbb{R}_+ | y_{MIN} \le y < \infty\}$, y_{MIN} is the minimum asset return observation governed by the power law, and α is the economic magnitude of the tail exponent.[1] Next, it can be shown that conditional moments $\left[y^k | y \ge y_{MIN}\right]$ are defined as

[1] We follow the notations of Clauset et al. (2009). To ensure better readability, indices (e.g., *t*, *b*, *W*, or *M*) are dropped here.

$$\left[y^{k}\,|y\geq y_{MIN}\right]=\frac{(\alpha-1)}{(\alpha-1-k)}y_{MIN}^{k}. \tag{5}$$

In line with White et al. (2008) and Clauset et al. (2009), maximum likelihood estimation (MLE) is employed to compute the tail exponent as

$$\ddot{\alpha}=1+N\left(\sum\nolimits_{i=1}^{N}\ln\left(\frac{y_i}{y_{MIN}}\right)\right)^{-1}, \tag{6}$$

where $\ddot{\alpha}$ denotes the MLE estimator and N denotes the number of sample observations exceeding y_{MIN}, that is, $y\geq y_{MIN}$. We see from Eq. (6) that the cutoff $y_{\min}$ is fundamentally important for the computation of the relevant power-law exponent. In line with Clauset et al. (2009), the cutoff $y_{\min}$ is assessed by means of the Kolmogorov–Smirnov (KS) distance D, which corresponds to the maximum distance between the empirical cumulative distribution function and the fitted power-law cumulative distribution function in the region $y\geq y_{\min}$, that is,

$$D=\max_{y\geq y_{\min}}\mid S(y)-P(y)\mid, \tag{7}$$

where $S(y)$ is the cumulative distribution function (CDF) of the data for observations with value at least $y_{\min}$, and $P(y)$ is the CDF implied by the fitted power-law model in the same region. The estimate of $y_{\min}$ is the value of $\ddot{y}_{\min}$ that minimizes D . Thus, the KS distance is used here as a fitting criterion for determining the optimal lower cutoff of the power-law region. To assess whether the fitted power-law model given by the parameter vector $(\ddot{\alpha},\ddot{y}_{\min})$ provides a reasonable description of the data, we further employ the goodness-of-fit test proposed by Clauset et al. (2009). This test generates a p-value by comparing the empirical KS distance with the distance measures obtained from comparable synthetic data sets drawn from the hypothesized model. In the present study, these p-values are reported descriptively across the simulated samples.[2]

3.3 Predicted Long-Range Dependence Derived From MMAR Simulations

Mandelbrot (2008) documented that the second wild trait that financial assets have in common is *long-range dependence* in otherwise random processes. A manifestation of this trait is, in the parlance of Mandelbrot (2008), the presence of decreasing correlations over time—however, the correlations decrease so slowly that they never seem to vanish completely, no matter how far back in time one goes.[3] To quantify the level of persistence in the simulated return processes of financial assets, we follow Mandelbrot (2008) by assessing the level of price persistence by means of estimated Hurst exponents derived from detrended fluctuation analysis (DFA), as proposed first

[2] The GoF test is detailed in Clauset et al. (2009).

[3] An illustrative example for the reasonability of slowly decreasing correlation is provided in Mandelbrot (2008, p. 184f).

by Peng et al. (1994), giving us the estimated Hurst exponent, $\ddot{H}$.[4] The DFA approach adopted here follows the same procedure as in Grobys (2023), employing linear detrending and the scale grid $s \in \{2,4,8,16,32,64,128,256\}$ for weekly data. For monthly data, the same procedure is used with the scale grid $s \in \{2,4,8,16,32,64\}$. The use of dyadic scale grids is motivated by the power-of-two construction underlying the MMAR simulations and follows Mandelbrot's (2008) scaling logic. Linear detrending corresponds to standard DFA(1), which is the conventional baseline implementation of the DFA methodology. As pointed out by Mandelbrot (2008), for independently distributed data, the ratio between numerator and denominator is 1:2, which corresponds to a Hurst exponent of $H = 0.50$. On other hand, $H > 0.50$ implies long-term dependence, whereas $H < 0.50$ implies antipersistence, which is characterized by the tendency to keep back on themselves.[5]

3.4 Predicted Scale Invariance Derived From MMAR Simulations

Mandelbrot (2008, p. 169) pointed out that "…economics is different. It lacks unquestioned mathematical laws to rely upon. Also, time, not space, is the scaling factor." If asset returns scale in time, we would expect asset returns to exhibit the same scaling factor across time frequencies as measured by the power-law exponent α. To explore whether the MMAR generates asset return data exhibiting scale invariance with respect to generated power-law behavior, for each given multiplicative cascade j, we implement two-sample split tests as follows:

$$H_0 : (\bar{\ddot{\alpha}}_{W,j} - \bar{\ddot{\alpha}}_{M,j}) = 0 \quad \text{vs.} \quad H_0 : (\bar{\ddot{\alpha}}_{W,j} - \bar{\ddot{\alpha}}_{M,j}) \neq 0,$$

where $\bar{\ddot{\alpha}}_{W,j}$ is the expected power-law exponent derived from weekly asset return data for a given cascade j, and $\bar{\ddot{\alpha}}_{M,j}$ is the expected power-law exponent derived from monthly asset return data for a given cascade j. The corresponding two-sample z-test statistic is defined as:

$$z = \frac{(\bar{\ddot{\alpha}}_{W,j} - \bar{\ddot{\alpha}}_{M,j})}{\sqrt{\left(\ddot{\sigma}^2_{\ddot{\alpha}_{W,j}} + \ddot{\sigma}^2_{\ddot{\alpha}_{M,j}}\right)/2}},$$

[4] The rationale for choosing DFA as opposed to rescaled range (R/S) analysis rests upon the study from Bassingthwaighte and Raymond (1994) in which it was shown that R/S analysis is subject to some bias. Specifically, the evidence derived from Bassingthwaighte and Raymond's (1994) study suggests that R/S analysis tends to give biased estimates of the Hurst exponent, too low for H>0.72 and too high for H<0.72.

[5] Note that $k\in ({2}^{r}\left|r\in \mathbb{N}\right.)$ must hold because if 1,024 weekly observations are required for the estimation, 5,120 daily observations are needed and, therefore, the multiplicative cascade used must exhibit $\ge \mathrm{5,120}$ observations. Consequently, earlier it was noted that 13 iterations are required for constructing the multiplicative cascade because ${2}^{13}=\mathrm{8,192}>\mathrm{5,120}$ as opposed to ${2}^{12}=\mathrm{4,096}<\mathrm{5,120}$, which would not result in a sufficient number of observations.

where $\ddot{\sigma}^2_{\ddot{\alpha}_{W,j}}$ and $\ddot{\sigma}^2_{\ddot{\alpha}_{M,j}}$ denote the variances for the estimated power-law exponents derived from weekly and monthly data, respectively, for a given multiplicative cascade j. If scale invariance for power-law behavior holds, the null hypothesis will not be rejected. We ascertain statistical significance using a common significance level of 5 percent.

Moreover, we hypothesize that scale invariance should also be manifested in invariance of the Hurst exponent because the power-law exponent and the Hurst exponent form—according to Mandelbrot (2008)—a *dual relationship*. Therefore, to analyze whether the MMAR generates asset return data that exhibit invariance with respect to long-range price persistence, for each given multiplicative cascade j, we furthermore implement two-sample split tests for the Hurst exponents as follows:

$$H_0 : (\overline{\ddot{H}}_{W,j} - \overline{\ddot{H}}_{M,j}) = 0 \text{vs.} H_0 : (\overline{\ddot{H}}_{W,j} - \overline{\ddot{H}}_{M,j}) \neq 0,$$

where $\overline{\ddot{H}}_{W,j}$ is the expected Hurst exponent derived from weekly asset return data for a given cascade j, and $\overline{\ddot{H}}_{M,j}$ is the expected Hurst exponent derived from monthly asset return data for a given cascade j. The corresponding two-sample z-test statistic is defined as:

$$z = \frac{(\overline{\ddot{H}}_{W,j} - \overline{\ddot{H}}_{M,j})}{\sqrt{\left(\ddot{\sigma}^2_{\ddot{H}_{W,j}} + \ddot{\sigma}^2_{\ddot{H}_{M,j}}\right)/2}},$$

where $\ddot{\sigma}^2_{\ddot{H}_{W,j}}$ and $\ddot{\sigma}^2_{\ddot{H}_{M,j}}$ denote the variances for the estimated Hurst exponents derived from weekly and monthly data, respectively, for a given multiplicative cascade j. If invariance for long-range dependence holds, the null hypothesis will not be rejected. We ascertain statistical significance using a common significance level of 5 percent.

3.5 Testing the MMAR Using Empirical Data: A Novel Joint Test for Testing for Discontinuity and Persistence

Can the MMAR explain power-law behavior and persistence observed for the returns on financial assets? An important—yet often overseen—aspect of financial assets is the impact of heavy tails: Specifically, in the presence of heavy tails, the vast part of an asset's return distribution appears to be relatively unimportant. In this regard, Cirillo and Taleb (2020, p. 606f) highlight that "the more fat-tailed a statistical distribution, the more the 'tail wags the dog'. That is to say, more statistical information resides in the extremes and less in the 'bulk'—the events of high frequency—where it becomes almost noise." Here, we are interested in testing whether the MMAR is capable of explaining the signals of the return-generating processes of financial assets that can—according to Mandelbrot (2008)—be described by their two key traits (i.e., discontinuity and long-range dependence). For a given MMAR specification j, let

$\overline{\ddot{\alpha}_j}$ and $\overline{\ddot{H}_j}$ denote the model-implied mean power-law and Hurst exponents obtained from the simulated return series, with corresponding simulation-based variances $\ddot{\sigma}^2_{\ddot{\alpha},j}$ and $\ddot{\sigma}^2_{\ddot{H},j}$. For an empirical test asset l, let $\widehat{\alpha}_l$ and $\widehat{H}_l$ denote the corresponding exponents estimated from the observed return data. The joint test then evaluates whether the empirical estimates are statistically consistent with the MMAR-implied predictions for a given model specification. To empirically test the MMAR, we propose the following joint test:

$$\lambda = \left(\begin{bmatrix} \overline{\ddot{\alpha}_j} - \widehat{\alpha}_l \end{bmatrix} \atop \begin{bmatrix} \overline{\ddot{H}_j} - \widehat{H}_l \end{bmatrix} \right)' \begin{pmatrix} \ddot{\sigma}^2_{\ddot{\alpha}_j} & 0 \\ 0 & \ddot{\sigma}^2_{\ddot{H}_j} \end{pmatrix}^{-1} \left(\begin{bmatrix} \overline{\ddot{\alpha}_j} - \widehat{\alpha}_l \end{bmatrix} \atop \begin{bmatrix} \overline{\ddot{H}_j} - \widehat{H}_l \end{bmatrix} \right), \tag{14}$$

where $\overline{\ddot{\alpha}_j}$ is the predicted power-law exponent associated with model j with corresponding variance $\ddot{\sigma}^2_{\ddot{\alpha}_j}$, and $\overline{\ddot{H}_j}$ is the corresponding predicted Hurst exponent with corresponding variance $\ddot{\sigma}^2_{\ddot{H}_j}$. Here, $\widehat{\alpha}_l$ and $\widehat{H}_l$ denote the estimated power-law exponent and Hurst exponent for some test asset l. Under the null hypothesis that the empirical power-law and Hurst exponents are equal to their MMAR-implied counterparts, and under the maintained assumption that the covariance between the two components is zero, the quadratic-form test statistic in Eq. (14) is asymptotically approximated by a $\chi^2(2)$ distribution. This result follows from standard asymptotic arguments for jointly standardized estimators.[6]

3.6 Testing for Invariance of Power-Law Behavior Over Time

Some recent literature argues that tail risk is time-varying and, consequently, the conditional power-law exponent derived from cross-sectional stock data has been proposed (Kelly, 2014; Kelly & Jiang, 2014). Hence, the question arises as to whether MMAR predictions would be in line with the literature on time-varying tail risk. To examine whether time variation in power-law behavior is in line with predictions derived from the MMAR, for each model specification j, the data on simulated weekly asset returns are split into two subsamples of equal length. Then, the following two-sample split z-test is implemented:

$$H_0 : (\overline{\ddot{\alpha}}_{WS1,j} - \overline{\ddot{\alpha}}_{WS2,j}) = 0 \text{vs.} H_0 : (\overline{\ddot{\alpha}}_{WS1,j} - \overline{\ddot{\alpha}}_{WS2,j}) \neq 0,$$

where $\overline{\ddot{\alpha}}_{WS1,j}$ is the expected power-law exponent derived from weekly asset return data for a given cascade j and subsample 1, whereas $\overline{\ddot{\alpha}}_{WS2,j}$ is the expected power-law exponent derived from weekly asset return data for a given cascade j and subsample 2.[7] The corresponding two-sample z-test statistic is defined as

[6] A more general statistical derivation of the distribution of the Wald test which is used in this joint test is detailed in Russell and MacKinnon (1993, p. 89).

[7] Obviously, the rationale for using weekly data as opposed to monthly data is that we have more observations for that frequency in order to estimate the power-law exponents.

$$z = \frac{(\overline{\ddot{\alpha}}_{WS1,j} - \overline{\ddot{\alpha}}_{WS2,j})}{\sqrt{\left(\ddot{\sigma}^2_{\ddot{\alpha}_{WS1,j}} + \ddot{\sigma}^2_{\ddot{\alpha}_{WS2,j}}\right)/2}},$$

where $\ddot{\sigma}^2_{\ddot{\alpha}_{WS1,j}}$ and $\ddot{\sigma}^2_{\ddot{\alpha}_{WS2,j}}$ denote the variances for the estimated power-law exponents derived from weekly data for a given subsample and a given multiplicative cascade j. If the time variation of power-law behavior is in line with predictions derived from the MMAR, the null hypothesis will be rejected. We ascertain statistical significance using a common significance level of 5 percent.

4 Results

4.1 Simulation-Based Evidence for Predicted Discontinuity Derived From the MMAR

This subsection reports results based on weekly simulated MMAR return data. To provide an illustrative example for the raw data used in this study, Fig. 2 plots one arbitrarily chosen time series of daily data for the MMAR derived from $p = 0.60$ (i.e., Model $j = 2$). For comparison, Fig. 3 plots drawings from the standard normal distribution. To make the time-series evolutions visually comparable, the data in

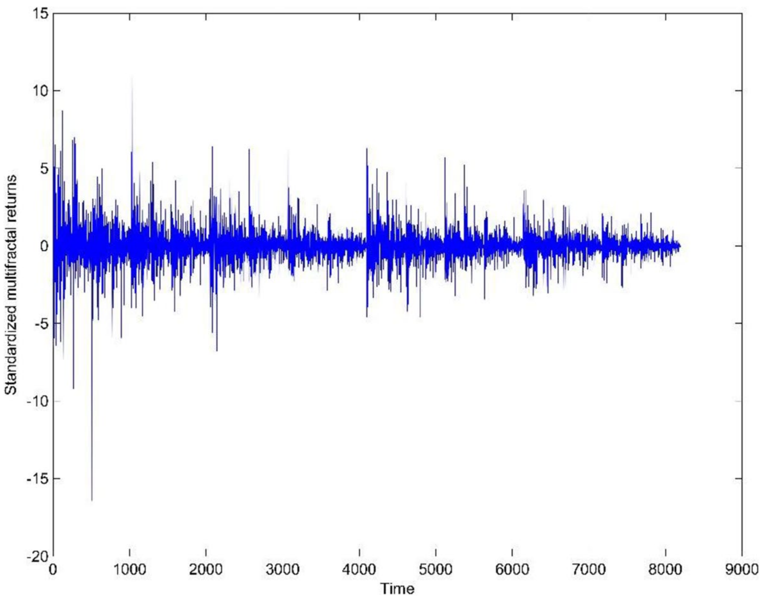

Fig. 2 Time series produced from the multifractal model of asset returns. This figure visualizes an arbitrarily chosen time series of daily data produced by the multifractal model of asset returns derived from a multiplicative cascade with $p = 0.60$. Note that the data are standardized to have zero mean and unit variance. The simulation uses 8192 drawings

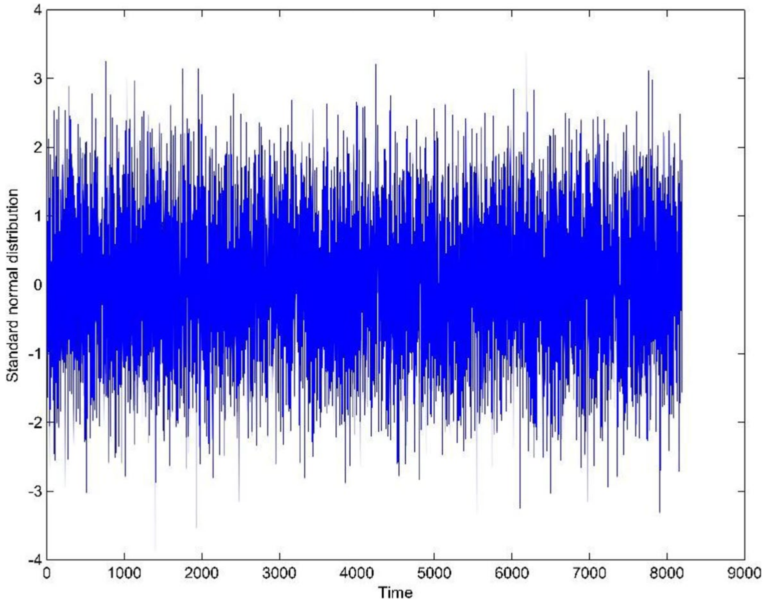

Fig. 3 Time series produced from the standard normal model. This figure visualizes drawings from the standard normal distribution. The simulation uses 8192 drawings

Fig. 2 were standardized so that $E(x) = 0$ and $VAR(x) = 1$. Moreover, both data sets exhibit 8,192 drawings. Figure 2 resembles closely the "cartoon" visualized in Mandelbrot (2008, p. 221). A visual comparison of Figs. 2 and 3 shows that asset return data generated from the MMAR exhibit the clustered and irregular behavior emphasized by Mandelbrot (2008), whereas the normal distribution does not. Unreported visualizations further indicate that as we move from Model 1 to Model 7, the return behavior generated by the MMAR becomes increasingly wild.

Tables 1, 2, 3, 4, 5, 6, and 7 report the descriptive statistics for Models 1–7 based on weekly simulated data and 1,000 simulated time series for each model specification j. Recall that Model 1 exhibits the lowest degree of time deformation, whereas Model 7 exhibits the highest. The results show that, as we move from Model 1 to Model 7, the expected power-law behavior becomes more extreme, manifested in decreasing expected power-law exponents. In particular, $E(\alpha) = \overline{\overline{\alpha}} = 5.27$ with $\sigma_\alpha = 1.33$ for Model 1, whereas $E(\alpha) = 1.83$ with $\sigma_\alpha = 0.22$ for Model 7. From Eqs. (5)–(7), this implies that Model 1 generates comparatively mild return data, whereas Model 7 generates substantially wilder return data. The same pattern is visible in other distributional properties reported in Tables 1, 2, 3, 4, 5, 6, and 7, including maxima, minima, and variances.

Tables 1, 2, 3, 4, 5, 6, and 7 also show that, on average, between 12 and 16 percent of the simulated return data are governed by a power law. The corresponding goodness-of-fit tests indicate that the power-law null model is not rejected for the majority of simulated return series. Overall, the weekly simulation evidence suggests that stronger time deformation, induced by higher values of p, is associated with

Table 1 Weekly multifractal return data derived from a multiplicative cascade with binominal bending and $p = 0.55$

Distribution	MAX	MIN	Mean	VAR	$\ddot{\alpha}$	$\ddot{x}_{min}$	% #PL state	p-value GoF	MAX #t in PL state	$\ddot{H}$
<2.5%	8.08	−15.57	−0.17	6.10	3.46	2.61	0.02	0.00	2	0.46
<5%	8.36	−14.56	−0.14	6.21	3.65	2.78	0.03	0.00	2	0.47
Median	10.49	−10.27	0.01	6.78	4.99	4.31	0.10	0.23	3	0.54
>95%	14.15	−8.27	0.14	7.41	7.77	6.23	0.25	0.91	7	0.60
>97.5%	15.12	−7.95	0.16	7.50	8.77	6.52	0.28	0.95	7	0.61
Min	6.73	−19.65	0.00	5.49	2.77	1.85	0.01	0.00	1	0.42
Max	22.27	−6.95	0.28	7.84	12.34	8.05	0.44	1.00	14	0.66
Mean	10.74	−10.66	0.00	6.79	5.27	4.37	0.12	0.33	3.58	0.54
Std.Dev	1.86	1.93	0.08	0.35	1.33	1.03	0.07	0.31	1.52	0.04

This Table reports the distribution of the maxima, minima, means, variances, estimated power-law exponent,$\ddot{\alpha}$, estimated cutoffs,$\ddot{x}_{min}$, percentage of observations governed by a power law with parametrization ($\ddot{\alpha}$,$\ddot{x}_{min}$), p-values of Clauset et al.'s (2009) goodness-of-fit tests, the maximum time lengths in power-law regimes measured in terms of consecutive observations, and the estimated Hurst exponents,$\ddot{H}$. The multifractal return data is based on a weekly frequency (1024 observations), and derived from a multiplicative cascade with binominal bending with $p = 0.55$.

Table 2 Weekly multifractal return data derived from a multiplicative cascade with binominal bending and $p = 0.60$

Distribution	MAX	MIN	Mean	VAR	$\ddot{\alpha}$	$\ddot{x}_{min}$	% #PL state	p-value GoF	MAX #t in PL state	$\ddot{H}$
<2.5%	12.83	−36.32	−0.22	9.47	2.71	2.43	0.03	0.00	2	0.48
<5%	13.52	−31.68	−0.17	9.87	2.84	2.71	0.04	0.00	2	0.49
Median	18.66	−18.73	0.00	11.16	3.68	4.85	0.12	0.20	5	0.55
>95%	30.89	−13.58	0.18	12.89	5.29	8.21	0.30	0.87	10	0.62
>97.5%	34.75	−12.75	0.21	13.26	5.70	8.91	0.33	0.94	12	0.63
Min	10.72	−50.70	−0.31	8.60	2.39	1.63	0.02	0.00	1	0.43
Max	59.49	−10.91	0.39	15.40	7.58	11.19	0.48	1.00	19	0.68
Mean	19.94	−20.18	0.00	11.23	3.81	5.04	0.14	0.31	5.26	0.55
Std.Dev	5.65	5.92	0.11	0.93	0.75	1.67	0.08	0.31	2.45	0.04

This Table reports the distribution of the maxima, minima, means, variances, estimated power-law exponent, $\ddot{\alpha}$, estimated cutoffs, $\ddot{x}_{min}$, percentage of observations governed by a power law with parametrization ($\ddot{\alpha}$, $\ddot{x}_{min}$), p-values of Clauset et al.'s (2009) goodness-of-fit tests, the maximum time lengths in power-law regimes measured in terms of consecutive observations, and the estimated Hurst exponents, $\ddot{H}$. The multifractal return data is based on a weekly frequency (1024 observations), and derived from a multiplicative cascade with binominal bending with $p = 0.60$

more pronounced discontinuity in returns, as reflected in lower expected power-law exponents.

4.2 Simulation-Based Evidence for Predicted Price Persistence Derived From the MMAR

Furthermore, we observe from Tables 1, 2, 3, 4, 5, 6, and 7 that as we move from Model 1 to Model 7, the level of expected data persistence increases. Specifically, we

Table 3 Weekly multifractal return data derived from a multiplicative cascade with binominal bending and $p = 0.65$

Distribution	MAX	MIN	Mean	VAR	$\ddot{\alpha}$	$\ddot{x}_{min}$	% #PL state	p-value GoF	MAX #t in PL state	$\ddot{H}$
<2.5%	21.73	−88.63	−0.30	17.17	2.26	2.10	0.03	0.00	2	0.49
<5%	23.11	−72.20	−0.23	17.84	2.35	2.43	0.03	0.00	3	0.51
Median	35.46	−36.47	0.01	21.84	2.98	5.51	0.13	0.21	6	0.58
>95%	68.25	−23.64	0.25	28.95	4.12	11.79	0.31	0.91	13	0.65
>97.5%	86.41	−21.83	0.29	31.71	4.45	13.20	0.36	0.96	16	0.66
Min	15.99	−126.09	−0.45	15.02	2.05	1.33	0.01	0.00	1	0.44
Max	154.28	−18.81	0.56	43.19	6.54	20.22	0.49	1.00	33	0.71
Mean	39.49	−40.27	0.01	22.42	3.07	6.08	0.14	0.31	6.71	0.58
Std.Dev	15.82	16.14	0.15	3.58	0.56	2.87	0.09	0.31	3.43	0.04

This Table reports the distribution of the maxima, minima, means, variances, estimated power-law exponent, $\ddot{\alpha}$, estimated cutoffs, $\ddot{x}_{min}$, percentage of observations governed by a power law with parametrization ($\ddot{\alpha}$, $\ddot{x}_{min}$), p-values of Clauset et al.'s (2009) goodness-of-fit tests, the maximum time lengths in power-law regimes measured in terms of consecutive observations, and the estimated Hurst exponents, $\ddot{H}$. The multifractal return data is based on a weekly frequency (1024 observations), and derived from a multiplicative cascade with binominal bending with $p = 0.65$

Table 4 Weekly multifractal return data derived from a multiplicative cascade with binominal bending and $p = 0.70$

Distribution	MAX	MIN	Mean	VAR	$\ddot{\alpha}$	$\ddot{x}_{min}$	% #PL state	p-value GoF	MAX #t in PL state	$\ddot{H}$
<2.5%	34.67	−202.05	−0.45	33.39	1.98	1.68	0.03	0.00	3	0.52
<5%	38.03	−158.57	−0.37	35.69	2.05	2.02	0.04	0.00	3	0.54
Median	68.30	−70.17	0.01	48.12	2.48	5.41	0.14	0.16	7	0.61
>95%	156.42	−40.21	0.37	85.62	3.29	14.54	0.33	0.87	17	0.68
>97.5%	199.24	−37.37	0.46	97.98	3.56	17.05	0.37	0.94	20	0.70
Min	26.46	−308.55	−0.77	27.63	1.85	1.06	0.01	0.00	2	0.47
Max	372.40	−28.82	0.80	177.56	4.87	27.96	0.49	1.00	26	0.74
Mean	78.73	−80.18	0.01	52.66	2.55	6.58	0.16	0.28	8.26	0.61
Std.Dev	40.86	40.86	0.23	16.47	0.39	4.05	0.09	0.30	4.24	0.05

This Table reports the distribution of the maxima, minima, means, variances, estimated power-law exponent, $\ddot{\alpha}$, estimated cutoffs, $\ddot{x}_{min}$, percentage of observations governed by a power law with parametrization ($\ddot{\alpha}$, $\ddot{x}_{min}$), p-values of Clauset et al.'s (2009) goodness-of-fit tests, the maximum time lengths in power-law regimes measured in terms of consecutive observations, and the estimated Hurst exponents, $\ddot{H}$. The multifractal return data is based on a weekly frequency (1024 observations), and derived from a multiplicative cascade with binominal bending with $p = 0.70$

observe that $E\left(H\right) = \overline{\ddot{H}} = 0.54$ with $\sigma_H = 0.04$ for Model 1, whereas $E\left(H\right) = 0.73$ with $\sigma_H = 0.08$ for Model 7. It is noteworthy that Mandelbrot (2008) argued that if $H = 0.50$, the return data are independent. From Tables 1 and 2 we observe that for Models 1 and 2, $\overline{\ddot{H}}$ is less than 2 standard deviations from $H = 0.50$. This implies that the MMAR data derived from multiplicative cascades with $p = 0.55$ or $p = 0.60$ produces return-generating processes that are, on expectation, independent. However, as the level of time deformation increases—manifested in higher values for

Table 5 Weekly multifractal return data derived from a multiplicative cascade with binominal bending and $p = 0.75$

Distribution	MAX	MIN	Mean	VAR	$\ddot{\alpha}$	$\ddot{x}_{min}$	% #PL state	p-value GoF	MAX #t in PL state	$\ddot{H}$
<2.5%	55.15	−442.91	−0.71	68.03	1.82	1.37	0.03	0.00	3	0.55
<5%	60.82	−364.61	−0.58	74.42	1.87	1.75	0.04	0.00	4	0.57
Median	127.74	−128.90	0.01	117.15	2.20	5.62	0.13	0.18	9	0.65
>95%	356.98	−63.84	0.61	293.05	2.82	18.80	0.31	0.90	18	0.73
>97.5%	456.02	−59.42	0.73	369.23	3.04	24.75	0.36	0.94	21	0.74
Min	41.09	−708.80	−1.33	51.28	1.68	0.70	0.01	0.00	2	0.50
Max	845.71	−42.16	1.19	791.22	3.88	42.35	0.50	1.00	46	0.80
Mean	154.45	−156.46	0.01	141.68	2.25	7.31	0.15	0.29	9.30	0.65
Std.Dev	98.92	97.41	0.37	77.54	0.31	5.79	0.09	0.31	5.00	0.05

This Table reports the distribution of the maxima, minima, means, variances, estimated power-law exponent, $\ddot{\alpha}$, estimated cutoffs, $\ddot{x}_{min}$, percentage of observations governed by a power law with parametrization ($\ddot{\alpha}$, $\ddot{x}_{min}$), p-values of Clauset et al.'s (2009) goodness-of-fit tests, the maximum time lengths in power-law regimes measured in terms of consecutive observations, and the estimated Hurst exponents, $\ddot{H}$. The multifractal return data is based on a weekly frequency (1024 observations), and derived from a multiplicative cascade with binominal bending with $p = 0.75$

Table 6 Weekly multifractal return data derived from a multiplicative cascade with binominal bending and $p = 0.80$

Distribution	MAX	MIN	Mean	VAR	$\ddot{\alpha}$	$\ddot{x}_{min}$	% #PL state	p-value GoF	MAX #t in PL state	$\ddot{H}$
<2.5%	77.98	−923.18	−1.21	138.83	1.69	1.04	0.02	0.00	3	0.58
<5%	92.78	−772.15	−1.02	150.06	1.71	1.22	0.03	0.00	4	0.60
Median	225.50	−220.47	0.01	305.96	1.99	5.46	0.12	0.15	10	0.69
>95%	787.24	−99.64	1.10	1077.71	2.47	24.48	0.30	0.86	21	0.77
>97.5%	957.06	−84.53	1.29	1498.45	2.70	32.00	0.33	0.93	23	0.78
Min	56.14	−1540.69	−2.25	79.54	1.56	0.35	0.01	0.00	2	0.53
Max	1820.49	−53.36	1.84	3435.10	4.30	53.19	0.51	1.00	47	0.85
Mean	296.29	−297.41	0.02	423.42	2.01	7.05	0.16	0.28	10.42	0.69
Std.Dev	228.90	222.83	0.63	351.82	0.26	7.55	0.09	0.30	5.56	0.05

This Table reports the distribution of the maxima, minima, means, variances, estimated power-law exponent, $\ddot{\alpha}$, estimated cutoffs, $\ddot{x}_{min}$, percentage of observations governed by a power law with parametrization ($\ddot{\alpha}$, $\ddot{x}_{min}$), p-values of Clauset et al.'s (2009) goodness-of-fit tests, the maximum time lengths in power-law regimes measured in terms of consecutive observations, and the estimated Hurst exponents, $\ddot{H}$. The multifractal return data is based on a weekly frequency (1024 observations), and derived from a multiplicative cascade with binominal bending with $p = 0.80$

p—return data on financial assets exhibit persistence: As an example, in line with Model 7, $E(H) = 0.73$ is 4.6 standard deviations above $H = 0.50$, suggesting a high level of price persistence.

4.3 Discontinuity and Price Persistence: A Joint Perspective

For illustrative purposes, we plot in Fig. 4 the estimated power-law exponents and estimated Hurst exponents for Models 1, 4, and 7 jointly in a multiple scat-

Table 7 Weekly multifractal return data derived from a multiplicative cascade with binominal bending and $p = 0.85$

Distribution	MAX	MIN	Mean	VAR	$\ddot{\alpha}$	$\ddot{x}_{min}$	% #PL state	p-value GoF	MAX #t in PL state	$\ddot{H}$
<2.5%	106.75	−1916.74	−2.15	261.78	1.57	0.55	0.03	0.00	3	0.62
<5%	133.92	−1617.46	−1.88	293.21	1.58	0.60	0.03	0.00	4	0.64
Median	357.16	−350.92	−0.02	824.27	1.82	4.08	0.12	0.13	10	0.73
>95%	1644.10	−153.26	1.98	4152.46	2.29	26.99	0.31	0.89	23	0.81
>97.5%	2017.70	−125.75	2.35	5872.95	2.41	31.83	0.32	0.96	24	0.82
Min	63.29	−3213.14	−3.69	180.06	1.43	0.11	0.02	0.00	2	0.56
Max	3738.73	−60.32	3.50	14,031.63	3.10	49.32	0.54	1.00	41	0.89
Mean	553.20	−551.93	0.02	1370.20	1.83	5.82	0.16	0.26	11.46	0.73
Std.Dev	512.31	492.61	1.14	1516.76	0.22	8.03	0.09	0.30	6.05	0.05

This Table reports the distribution of the maxima, minima, means, variances, estimated power-law exponent, $\ddot{\alpha}$, estimated cutoffs, $\ddot{x}_{min}$, percentage of observations governed by a power law with parametrization ($\ddot{\alpha}$, $\ddot{x}_{min}$), p-values of Clauset et al.'s (2009) goodness-of-fit tests, the maximum time lengths in power-law regimes measured in terms of consecutive observations, and the estimated Hurst exponents, $\ddot{H}$. The multifractal return data is based on a weekly frequency (1024 observations), and derived from a multiplicative cascade with binominal bending with $p = 0.85$

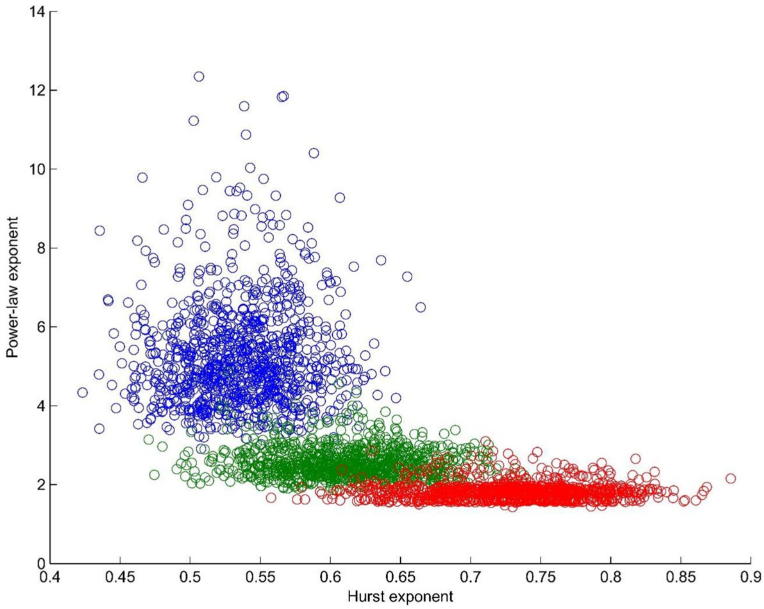

Fig. 4 Power-law exponents and Hurst exponents predicted by various models. This figure plots power-law exponents and Hurst exponents for Models 1, 4, and 7 jointly in a multiple scatter plot. In this figure, the blue data cloud corresponds to the vectors $(\ddot{\alpha}_{1,1}, \ddot{H}_{1,1})$, ..., $(\ddot{\alpha}_{1,1000}, \ddot{H}_{1,1000})$ for $j = 1$ with $p = 0.55$, the green data cloud corresponds to the vectors $(\ddot{\alpha}_{4,1}, \ddot{H}_{4,1})$, ..., $(\ddot{\alpha}_{4,1000}, \ddot{H}_{4,1000}$) for $j = 4$ with $p = 0.70$, whereas the red data cloud corresponds to the vectors $(\ddot{\alpha}_{7,1}, \ddot{H}_{7,1})$, ..., $(\ddot{\alpha}_{7,1000}, \ddot{H}_{7,1000})$ for $j = 7$ with $p = 0.85$

ter plot. In Fig. 4, the blue data cloud corresponds to the vectors $(\ddot{\alpha}_{1,1}, \ddot{H}_{1,1})$, …, $(\ddot{\alpha}_{1,1000}, \ddot{H}_{1,1000})$ for $j = 1$ with $p = 0.55$, the green data cloud corresponds to the vectors $(\ddot{\alpha}_{4,1}, \ddot{H}_{4,1})$, …, $(\ddot{\alpha}_{4,1000}, \ddot{H}_{4,1000})$ for $j = 4$ with $p = 0.70$, and the red data cloud corresponds to the vectors $(\ddot{\alpha}_{7,1}, \ddot{H}_{7,1})$, …, $(\ddot{\alpha}_{7,1000}, \ddot{H}_{7,1000})$ for $j = 7$ with $p = 0.85$. From visual inspection of Fig. 4 at least three interesting insights arise:

First, for each given data cloud the variation of the Hurst exponents does not seem to be dependent on the power-law exponents. Specifically, estimated correlations, $\widehat{\rho}(\ddot{\alpha}_j, \ddot{H}_j)$, for Models 1–7 vary between $\widehat{\rho}(\ddot{\alpha}_4, \ddot{H}_4) = -0.07$, and $\widehat{\rho}(\ddot{\alpha}_1, \ddot{H}_1) = 0.05$. Because the $\chi^2(2)$ reference distribution developed in Section 3.5 relies on a zero-covariance assumption between the simulated power-law and Hurst exponents, we tested the correlation between estimated power-law exponent and Hurst exponent for each MMAR specification for statistical significance using the Pearson correlation test statistics. The estimated correlations are close to zero and are statistically insignificant in nearly all cases, supporting the maintained approximation used in the conjoint test. Specifically, for Models 1–7, the estimated Pearson correlation test statistics are $t = \{1.4451, -0.1636, -1.6979, -2.1727, -1.8887, -1.1548, 0.4848\}$, with corresponding p-values $\{0.1487, 0.8701, 0.0898, 0.0300, 0.0592, 0.2485, 0.6279\}$. Overall, the estimated correlations are uniformly small in magnitude. Although Model 4 yields a p-value below 5 percent, this isolated finding is not robust to a Bonferroni adjustment for multiple testing, under which the adjusted critical level is 0.0071.

Second, we observe from Fig. 4 that the blue data cloud and the red data cloud are virtually non-overlapping. This implies that discontinuity and long-range dependence are features that are apparently related to specific model parametrizations depending on p. This is an interesting result because it shows that the level of price persistence depends to a high degree on the multiplicative cascade and does not necessarily depend solely on the fractional Brownian motion. Third, we see from Table 1 in association with Table 7 that $\overline{\ddot{H}}_7$ exceeds $\overline{\ddot{H}}_1$ by 4.75 standard deviations (i.e., $4.75\sigma_{\overline{\ddot{H}}_1}$), whereas $\overline{\ddot{H}}_1$ is 3.80 standard deviations (i.e., $3.80\sigma_{\overline{\ddot{H}}_7}$) below $\overline{\ddot{H}}_7$. This strongly suggests that these two models indeed produce, on expectation, model-specific persistence structures. Since the increments of the returns x_t are according to Eq. (1), z_t and ε_t, where $\varepsilon_t \sim IIDN(0,1)$—which are independent increments—our results suggest that asset price persistence is in the present study's model framework solely explained by differences in z_t—the multiplicative cascade. Specifically, the more concentrated the distribution of the multiplicative cascade, the higher is the level of price persistence.

4.4 Does the MMAR Predict Scale Invariance?

This subsection compares weekly and monthly simulated MMAR return data. According to Mandelbrot (2008), scale invariance implies that power-law behavior does not change as the time frequency changes. To explore, this issue, we estimate the power-law exponents and Hurst exponents for MMAR specifications derived from monthly data. The corresponding distributional properties are reported in Tables 12, 13, 14, 15, 16, 17, and 18 in the Appendix. Comparing Tables 1, 2, 3, 4, 5, 6, and

7 with Tables 12, 13, 14, 15, 16, 17, and 18 shows that the expected power-law exponents and expected Hurst exponents are close to each other across weekly and monthly frequencies.

Panel A of Table 8 reports the z-tests for whether discontinuity, manifested in model-specific expected power-law behavior, is invariant across time frequencies. The estimated z-statistics are all well below $\mid 1.96 \mid$, so the null hypothesis of scale-invariant power-law behavior is not rejected for any $j \in \{1,2,\ldots,7\}$. Thus, the MMAR predicts that power-law behavior is statistically the same across weekly and monthly time frequencies. As a robustness check, Panel B of Table 8 reports the corresponding z-tests for the Hurst exponents. Again, the estimated z-statistics are all well below $\mid 1.96 \mid$, indicating that the null hypothesis of scale-invariant price persistence is not rejected for any model specification. Taken together, the evidence in Table 8 supports the view that the MMAR predicts scale invariance for both discontinuity and long-range dependence.

4.5 4.5. An Empirical Investigation of a Joint Test to Assess Whether the MMAR is Capable of Describing Discontinuity and Price Persistence Across the Returns on Otherwise Unrelated Asset Markets

This subsection reports results based on empirical weekly asset-return data. To test whether observed discontinuity and price persistence are in line with MMAR predictions, we employ weekly returns on five key financial asset markets as test assets: the U.S. S&P 500, the USD/GBP exchange rate, gold futures, crude oil futures, and Bitcoin. Extending Calvet and Fisher (2002), the analysis therefore covers not only equity and foreign exchange markets, but also commodities and cryptocurrencies. The sample period runs from January 3, 2016 until September 22, 2024.

For the returns on each asset, we estimate both the asset-specific power-law exponent and the asset-specific Hurst exponent. We then implement the test statistic introduced in Section 3.5 for each asset and for the various MMAR model specifications. The results are reported in Table 9. For illustration, consider Bitcoin. Table 9 shows that the estimated power-law exponent is $\widehat{\alpha}_{BTC} = 3.1531$, whereas the estimated Hurst exponent is $\widehat{H}_{BTC} = 0.6219$. The corresponding joint test statistics indicate that the null hypothesis is not rejected for Models 2–4, with the smallest test statistic obtained for Model 3. Thus, the MMAR is capable of accounting for the observed discontinuity and persistence in Bitcoin returns under several nearby model specifications.

Overall, Panel B of Table 9 shows that for the vast majority of the five test assets, the null hypothesis is not rejected for Models 1–4. This indicates that the benchmark MMAR and its nearby extensions are capable of describing the discontinuity and price persistence observed for the returns on these otherwise unrelated asset markets. Table 9 also shows that the benchmark model proposed by Mandelbrot (2008), corresponding to Model 2, performs well across all five assets and is therefore broadly consistent with the empirical return dynamics considered in this study. Figure 5 visualizes the power-law exponents and Hurst exponents in α/H space predicted by the multifractal model of asset returns with p=0.60. The figure shows that the empirical estimates lie within the simulated scatter.

Table 8 Testing for invariance across time frequencies

To explore whether the MMAR generates asset return data that exhibiting scale invariance with respect to generated power-law behavior, for each given multiplicative cascade$j$, two-sample split tests are implemented as follows:

$H_0 : (\overline{\ddot{\alpha}}_{W,j} - \overline{\ddot{\alpha}}_{M,j}) = 0$ vs. $H_0 : (\overline{\ddot{\alpha}}_{W,j} - \overline{\ddot{\alpha}}_{M,j}) \neq 0$,

where $\overline{\ddot{\alpha}}_{W,j}$ is the expected power-law exponent derived from weekly asset return data for a given cascade$j$, and$\overline{\ddot{\alpha}}_{M,j}$is the expected power-law exponent derived from monthly asset return data for a given cascade$j$. The corresponding two-sample z-test statistics are defined as:

$$z = \frac{(\overline{\ddot{\alpha}}_{W,j} - \overline{\ddot{\alpha}}_{M,j})}{\sqrt{\left(\ddot{\sigma}^2_{\ddot{\alpha}_{W,j}} + \ddot{\sigma}^2_{\ddot{\alpha}_{M,j}}\right)/2}},$$

where $\ddot{\sigma}^2_{\ddot{\alpha}_{W,j}}$ and $\ddot{\sigma}^2_{\ddot{\alpha}_{M,j}}$ denote the variances for the estimated power-law exponents derived from weekly, respectively, monthly data, for a given multiplicative cascade

j. If scale invariance for power-law behavior holds, the null hypothesis will not be rejected. Moreover, to analyze whether the MMAR generates asset return data that exhibits invariance with respect to long-range persistence, for each given multiplicative cascade j, further two-sample split tests for the Hurst exponents are implemented as follows:

$H_0 : (\overline{\ddot{H}}_{W,j} - \overline{\ddot{H}}_{M,j}) = 0$ vs. $H_0 : (\overline{\ddot{H}}_{W,j} - \overline{\ddot{H}}_{M,j}) \neq 0$,

where $\overline{\ddot{H}}_{W,j}$ is the expected Hurst exponent derived from weekly asset return data for a given cascade j, and $\overline{\ddot{H}}_{M,j}$ is the expected Hurst exponent derived from monthly asset return data for a given cascade j. The corresponding two-sample z-test statistics are defined as:

$$z = \frac{(\overline{\ddot{H}}_{W,j} - \overline{\ddot{H}}_{M,j})}{\sqrt{\left(\ddot{\sigma}^2_{\ddot{H}_{W,j}} + \ddot{\sigma}^2_{\ddot{H}_{M,j}}\right)/2}},$$

where $\ddot{\sigma}^2_{\ddot{H}_{W,j}}$ and $\ddot{\sigma}^2_{\ddot{H}_{M,j}}$ denote the variances for the estimated Hurst exponents derived from weekly, respectively, monthly data, for a given multiplicative cascade j. If invariance for long-range dependence holds, the null hypothesis will not be rejected. A significance of 5% is used to ascertain statistical significance

Panel A. Testing power-law exponents for invariance

Table 8 (continued)

Probability p	$\ddot{\overline{\alpha}}_W$	$\ddot{\overline{\alpha}}_M$	$\ddot{\sigma}_{W\ddot{\overline{\alpha}}}$	$\ddot{\sigma}_{M\ddot{\overline{\alpha}}}$	$(\ddot{\overline{\alpha}}_W - \ddot{\overline{\alpha}}_M)$	$\ddot{\sigma}_{(\ddot{\overline{\alpha}}_W - \ddot{\overline{\alpha}}_M)}$	z-statistic
0.55	5.27	4.78	1.33	1.49	0.49	1.41	0.35
0.60	3.81	3.68	0.75	0.98	0.13	0.87	0.15
0.65	3.07	2.98	0.56	0.67	0.09	0.62	0.15
0.70	2.55	2.56	0.39	0.56	−0.01	0.48	−0.02
0.75	2.25	2.24	0.31	0.43	0.01	0.37	0.03
0.80	2.01	2.03	0.26	0.35	−0.02	0.31	−0.06
0.85	1.83	1.84	0.22	0.28	−0.01	0.25	−0.04
Panel B. Testing Hurst exponents for invariance							
Probability p	$\ddot{\overline{H}}_W$	$\ddot{\overline{H}}_M$	$\ddot{\sigma}_{W\ddot{\overline{H}}}$	$\ddot{\sigma}_{M\ddot{\overline{H}}}$	$(\ddot{\overline{H}}_W - \ddot{\overline{H}}_M)$	$\ddot{\sigma}_{(\ddot{\overline{H}}_W - \ddot{\overline{H}}_M)}$	z-statistic
0.55	0.54	0.56	0.04	0.06	−0.02	0.05	−0.39
0.60	0.55	0.57	0.04	0.06	−0.02	0.05	−0.39
0.65	0.58	0.59	0.04	0.07	−0.01	0.06	−0.18
0.70	0.61	0.62	0.05	0.07	−0.01	0.06	−0.16
0.75	0.65	0.66	0.05	0.07	−0.01	0.06	−0.16
0.80	0.69	0.70	0.05	0.08	−0.01	0.07	−0.15
0.85	0.73	0.74	0.05	0.08	−0.01	0.07	−0.15

Table 9 Testing the predicted power-law behavior and persistence generated by the MMAR for various financial assets

To test the MMAR predictions, weekly log-return data on the following assets were used as test assets: the S&P 500, the USD/GBP exchange rate, gold futures, crude oil futures, and Bitcoin. The weekly sample period runs from January 3, 2016 to September 22, 2024. In addition, monthly log-return data on the S&P 500, the USD/GBP exchange rate, gold futures, and crude oil futures were used for a robustness analysis. The monthly sample period runs from October 1981 to March 2026. Panel A (C) of this table reports the estimated power-law exponents and Hurst exponents for the test assets, together with the corresponding standard deviations, for weekly (monthly) data. To assess whether the MMAR is capable of describing discontinuity and price persistence in the observed return data, the joint test proposed in this study is implemented as:

$$\lambda = \left(\begin{bmatrix} \overline{\ddot{\alpha}}_j - \widehat{\alpha}_l \\ \overline{\ddot{H}}_j - \widehat{H}_l \end{bmatrix} \right)' \begin{pmatrix} \ddot{\sigma}^2_{\ddot{\alpha}_j} & 0 \\ 0 & \ddot{\sigma}^2_{\ddot{H}_j} \end{pmatrix}^{-1} \left(\begin{bmatrix} \overline{\ddot{\alpha}}_j - \widehat{\alpha}_l \\ \overline{\ddot{H}}_j - \widehat{H}_l \end{bmatrix} \right),$$

where $\overline{\ddot{\alpha}}_j$ is the predicted power-law exponent associated with cascade j as $\overline{\ddot{\alpha}}_j$ with corresponding variance $\ddot{\sigma}^2_{\ddot{\alpha}_j}$, and $\overline{\ddot{H}}_j$ is the predicted Hurst exponent associated with cascade j with corresponding variance $\ddot{\sigma}^2_{\ddot{H}_j}$. Here ,$\widehat{\alpha}_l$ and $\widehat{H}_l$ denote the estimated power-law exponent and Hurst exponent for test asset . Provided $cov(\overline{\ddot{\alpha}}_j, \overline{\ddot{H}}_j) = 0$, the test statistic λ is under the null hypothesis distributed as $\chi^2(2)$. Panel B (D) of this table reports the estimated joint-test statistics for weekly (monthly) data. Using a significance level of 5 percent, the null hypothesis is not rejected for $\widehat{\lambda} < 5.99$. **Bold** values indicate the optimal model

Panel A. Estimated power-law exponents and Hurst exponents

Asset	S&P500	USD/GBP	Gold Futures	Crude Oil Futures	Bitcoin
$\widehat{\alpha}$	3.0644	4.2671	3.6957	3.8984	3.1531
$\widehat{\sigma}_{\widehat{\alpha}}$	0.1911	0.4109	0.2871	0.3433	0.1989
y_{MIN}	0.0206	0.0175	0.0232	0.0717	0.1001
$\widehat{H}$	0.4869	0.5322	0.5217	0.5951	0.6219
$\widehat{\sigma}_{\widehat{H}}$	0.0407	0.0255	0.0389	0.0440	0.0304
Sample starts	01/03/2016	01/03/2016	01/03/2016	01/03/2016	01/03/2016
Sample ends	09/22/2024	09/22/2024	09/22/2024	09/22/2024	09/22/2024
T	456	456	456	456	456
N	127	68	95	77	127
% (N)	27.85%	14.91%	20.83%	16.89%	27.85%

Panel B. Estimated test statistics for joint tests

Model j/Asset l	S&P500	USD/GBP	Gold Futures	Crude Oil Futures	Bitcoin
1	4.5124	0.6066	1.6104	2.9610	6.7256
2	**3.4768**	**0.5695**	**0.5238**	**1.2851**	3.9981

Table 9 (continued)

3	5.4174	5.9977	3.3727	2.3308	**1.1193**
4	7.8011	21.8060	11.7488	12.0427	2.4480
5	17.5423	47.8888	28.3330	29.4806	8.8027
6	32.9460	85.3228	53.3652	56.3547	21.1846
7	55.1213	138.3660	89.2737	95.6734	40.8435
Panel C. Estimated power-law exponents and Hurst exponents using monthly data					
Asset	S&P500	USD/GBP	Gold Futures	Crude Oil Futures	
$\widehat{\alpha}$	5.4541	4.4896	3.2796	4.2641	
$\widehat{\sigma}_{\widehat{\alpha}}$	0.9722	0.5245	0.2044	0.3532	
y_{MIN}	8.9772	4.5738	9.4841	6.1352	
$\widehat{H}$	0.5654	0.5190	0.5083	0.5242	
$\widehat{\sigma}_{\widehat{H}}$	0.0132	0.0332	0.0353	0.0189	
Sample starts	31/10/1981	31/10/1981	31/10/1981	31/10/1981	
Sample ends	31/3/2026	31/3/2026	31/3/2026	31/3/2026	
T	534	534	534	534	
N	23	48	134	91	
% (N)	4.30%	8.99%	25.09%	17.04%	
Panel D. Estimated joint-test statistics for monthly data					
Model j/Asset l	S&P500	USD/GBP	Gold Futures	Crude Oil Futures	
1	**0.2128**	**0.5049**	1.7565	**0.4759**	
2	3.2831	1.4050	**1.2244**	0.9379	
3	13.7594	6.1054	1.5622	4.5568	
4	27.3170	13.9548	4.1975	11.1331	
5	57.6968	31.4273	10.5417	25.9214	
6	98.5407	54.5037	18.4890	45.5735	
7	171.3669	97.1771	34.8226	82.2288	

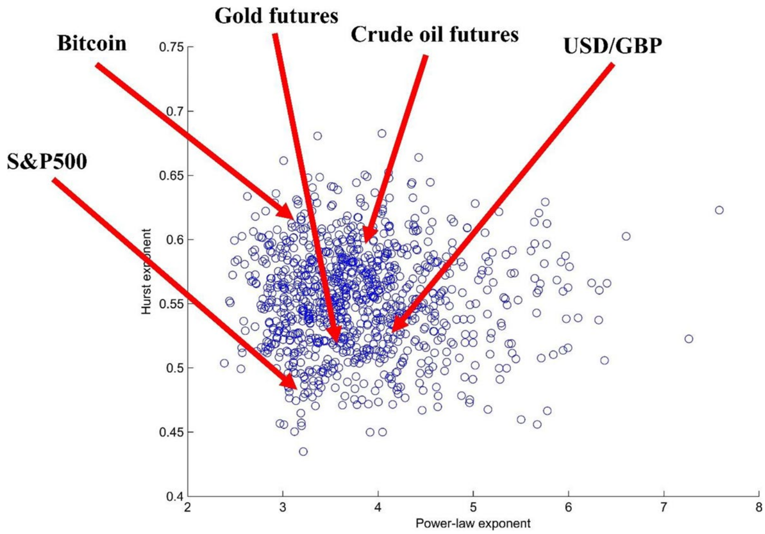

Fig. 5 This figure plots the estimated power law exponents and associated Hurst exponents for five financial asset markets in the α/H space predicted from the multifractal model of asset returns with p = 0.60

As a robustness check, the conjoint test was also implemented using monthly log-return data on the U.S. S&P 500, USD/GBP exchange rate, gold futures, and crude oil futures. The corresponding results are reported in Panels C and D of Table 9. Overall, the evidence suggests that the MMAR with $p = 0.55$ is not rejected for any of the four monthly asset-return series and provides the best fit for the U.S. S&P 500, USD/GBP exchange rate, and crude oil futures. The benchmark MMAR with $p = 0.60$ is likewise not rejected for all four markets and is the preferred specification for gold futures. Hence, the monthly-data evidence broadly confirms the conclusions drawn from the weekly analysis and indicates that the benchmark MMAR and its nearby specification remain capable of describing discontinuity and price persistence across different time frequencies.

4.6 Does the MMAR Predict Invariance of Power-Law Behavior Over Time?

This subsection uses weekly simulated MMAR data split into two non-overlapping subsamples. Some recent literature argues that tail risk is time-varying. To examine whether such time variation is in line with predictions derived from the MMAR, the simulated weekly return data are split into two subsamples of equal length for each model specification j. The corresponding distributional properties are reported in Tables 19, 20, 21, 22, 23, 24, 25, 26, 27, 28, 29, 30, 31, and 32 in the Appendix, while the z-tests are summarized in Table 10.

Panel A of Table 10 reports the z-tests for whether expected power-law exponents differ across the two subsamples. The estimated z-statistics are all below $|\ 1.96\ |$, indicating that the null hypothesis of equal expected power-law exponents is not rejected

Table 10 Testing for invariance of power law exponents over time

To examine whether changes in power-law behavior are in line with the MMAR, for each given multiplicative cascade j, the data on simulated weekly asset returns are split into two subsamples of equal length, and then, the following two sample split z-tests are implemented:

$H_0 : (\overline{\ddot{\alpha}}_{WS1,j} - \overline{\ddot{\alpha}}_{WS2,j}) = 0$ vs. $H_0 : (\overline{\ddot{\alpha}}_{WS1,j} - \overline{\ddot{\alpha}}_{WS2,j}) \neq 0$,

where $\overline{\ddot{\alpha}}_{WS1,j}$ is the expected power-law exponent derived from weekly asset return data for a given cascade j and subsample 1, whereas $\overline{\ddot{\alpha}}_{WS2,j}$ is the expected power-law exponent derived from weekly asset return data for a given cascade j and subsample 2. The corresponding two-sample z-test statistics are defined as:

$$z = \frac{(\overline{\ddot{\alpha}}_{WS1,j} - \overline{\ddot{\alpha}}_{WS2,j})}{\sqrt{\left(\ddot{\sigma}^2_{\ddot{\alpha}_{WS1,j}} + \ddot{\sigma}^2_{\ddot{\alpha}_{WS2,j}}\right)/2}},$$

where $\ddot{\sigma}^2_{\ddot{\alpha}_{WS1,j}}$ and $\ddot{\sigma}^2_{\ddot{\alpha}_{WS2,j}}$ denote the variances for the estimated power-law exponents derived from weekly data, for a given subsample and a given multiplicative cascade j. If changes in power-law behavior are in line with the MMAR, the null hypothesis will be rejected. A significance of 5% is used to ascertain statistical significance

Probability p	$\overline{\ddot{\alpha}}_{S1}$	$\overline{\ddot{\alpha}}_{S2}$	$\ddot{\sigma}_{\overline{\ddot{\alpha}}S1}$	$\ddot{\sigma}_{\overline{\ddot{\alpha}}S2}$	$(\overline{\ddot{\alpha}}_{S1} - \overline{\ddot{\alpha}}_{S2})$	$\ddot{\sigma}_{(\overline{\ddot{\alpha}}_{S1} - \overline{\ddot{\alpha}}_{S2})}$	z-statistic
0.55	5.06	5.06	1.50	1.50	0.00	1.50	0.00
0.60	3.73	3.77	0.89	0.88	−0.04	0.89	−0.04
0.65	3.00	3.00	0.60	0.61	0.00	0.61	0.00
0.70	2.53	2.54	0.46	0.45	−0.01	0.46	−0.02
0.75	2.22	2.24	0.35	0.37	−0.02	0.36	−0.06
0.80	2.01	2.01	0.32	0.30	0.00	0.31	0.00
0.85	1.84	1.84	0.26	0.26	0.00	0.26	0.00

for any model specification. Hence, the MMAR does not predict statistically significant time variation in expected power-law behavior at the weekly frequency.

Panel B of Table 10 reports the corresponding results for the Hurst exponents. Again, the estimated z-statistics remain below conventional critical values, indicating that the null hypothesis of equal expected Hurst exponents across subsamples is not rejected. Taken together, the evidence suggests that the MMAR predicts invariance over time not only for discontinuity, as measured by power-law exponents, but also for price persistence, as measured by Hurst exponents.

5 Discussion

5.1 How do the Results Line Up With Earlier Research?

Exploring the performance of the MMAR through the lenses of describing the evolution of financial asset prices, Calvet and Fisher (2002) found evidence for multifractality in the moment-scaling behavior of Deutsche mark/U.S. dollar exchange rates, the value-weighted CRSP Index, and five U.S. stocks (ADM, GM, Lockheed-Martin, Motorola, and UAL). Extending the study of Calvet and Fisher (2002), the present study takes a novel perspective by exploring the predicted discontinuity and price persistence of financial asset returns derived from simulations of various MMAR model specifications. The rationale is here Mandelbrot's (2008) argument that discontinuity and price persistence are the two key characteristic traits of financial assets.[8] Using the distributions for the power-law exponents and Hurst exponents derived from MMAR simulations, we proposed a statistical test designed to test whether the MMAR is capable of describing the two key characteristic traits jointly.[9]

Notably, in line with the study of Grobys (2023) which investigates discontinuity and price persistence in the realized variance processes of financial assets, our findings derived from asset return processes suggest that for any MMAR specification, power-law exponents and Hurst exponents are uncorrelated. Furthermore, our findings indicate that power-law behavior in the returns on financial assets becomes "wilder" as we move from an MMAR specification with $p = 0.55$ to a specification with $p = 0.85$, which is also in line with Grobys (2023), who documented that $E(\alpha) = 3.72$ for an MMAI specification with $p = 0.55$ and $E(\alpha) = 1.84$ for an MMAI specification with $p = 0.70$. The corresponding figures in the context of the present research are $E(\alpha) = 5.27$ and $E(\alpha) = 2.55$, respectively.[10]

[8] Note also that Cirillo and Taleb's (2020) stress that, in the presence of heavy tails, the statistical signal of return distribution resides in the tails of distributions—the part of the asset return distribution governed by a power-law process. As a result, our test is designed to examine whether the MMAR is capable of describing the signal of return-generating processes.

[9] The rationale for proposing a joint test is Mandelbrot's (2008) argument that power-law exponent and Hurst exponent form a *dual relationship*. Note that our findings indicated that, in fact, every MMAR specification produces model-specific power-law exponents accompanied by model-specific Hurst exponents.

[10] Here, we refer to our results derived from weekly data.

It is interesting to note that MMAR and MMAI exhibit considerable differences. As an example, the benchmark model specification in Grobys' (2023) study is derived from Mandelbrot's (2008) "cartoon"—a model incorporating a multiplicative cascade based on binominal bending with $p = 0.60$. Whereas the MMAI predicts $E(\alpha) = 2.61$ and $E(H) = 0.88$, the MMAR that would produce a similar power-law behavior required a model specification of $p = 0.70$, giving us $E(\alpha) = 2.55$ and $E(H) = 0.61$. Notably, despite generating similar power-law behaviors, the predicted persistence is considerably higher for the MMAI. This feature, however, aligns nicely with real world observations because in financial markets volatility is more persistence than asset returns.[11] In fact, MMAR model specifications with $p = 0.55$, or $p = 0.60$ suggest that asset return processes are, on expectation, memoryless because, statistically, $E(H) = 0.50$ cannot be rejected for these model specifications. On the other hand, Grobys' (2023) MMAI with model specification $p = 0.55$ suggests a high level of variance persistence manifested in $E(H) = 0.80$.

Furthermore, some literature suggests that tail behavior is subject to tail dependency, as postulated in studies by Kelly (2014) and Kelly and Jiang (2014). We would like to argue that time-dependent power-law behavior would be a somewhat surprising finding against the background of Mandelbrot's (2008) favoritism of invariance. Unsurprisingly, simulation-based evidence documented in the present study does not support the claim that power-law behavior in the returns on financial assets is regime-switching. On the contrary, our findings suggest that the MMAR predicts that the power-law exponent is not only constant across time frequencies but also constant over time. This result aligns with the recent empirical findings documented in Grobys (2024), suggesting that realized foreign exchange rate variances are subject to total invariance—that is, power-law behavior of realized foreign exchange rate variances is invariant across time frequencies and invariant over time.

5.2 What are the Implications?

Whereas earlier research found evidence for that the moment scaling behavior of foreign exchange rates and equities are in line with predictions from the MMAR (Calvet & Fisher, 2002), the evidence derived from our proposed joint tests suggests that Mandelbrot's (2008) "cartoon" is capable of explaining the power-law behavior and price persistence observed across otherwise unrelated asset market, including Bitcoin—an asset class that is well-known to be subject to reoccurring extreme events and bubble formations. The novel economic implication of our result is that the trading time—which Mandelbrot et al. (1997) and Mandelbrot (2008) interpret as "deformed clock time"—required to mimic the level of discontinuity and price persistence empirically observed for five otherwise unrelated asset markets—the market for U.S. equities, USD/GBP foreign exchange rates, gold futures, crude oil futures and Bitcoin—is governed by a common law manifested in a universal multiplicative

[11] For instance, a recent study by Grobys et al. (2023) estimated the Hurst exponent for the overall U.S. equity market over the September 1934 to December 2019 sample. The authors documented that the estimated Hurst exponent for this sample is exactly $\widehat{H} = 0.50$ suggesting a memoryless process.

cascade derived binominal bending of time with $p = 0.60$.[12] Since well-established literature suggests that power-law behavior of financial assets are manifestations of herding behavior (e.g., Lux, 1995; Lux & Marchesi, 1999), the results derived from the present study imply that the herding behaviors across otherwise unrelated asset markets must share some common source.

This is indeed an intriguing finding because the participators active in the market for foreign exchanges are very different from market participators in the market for equities or cryptocurrencies. For example, Menkhoff et al. (2012) argue that foreign exchange rate markets are populated largely by sophisticated professional investors, and there are no natural short-selling constraints. The other extreme spectrum, in the markets for financial assets investigated in the present study, forms Bitcoin: Whereas the vast majority of traders are retail traders—as opposed to professional investors—Foley et al. (2019) document that 46% of bitcoin transactions can be traced back to some form of criminal activity. Yet, despite of exhibiting a very different client base of traders, our results derived from the MMAR imply that the herding behavior producing power-law regimes is governed by the same law manifested in a universal multiplicative cascade derived from binominal bending of time with $p = 0.60$.

An important issue concerns the economic interpretation of time deformation, z_t, in the MMAR. Although Mandelbrot (2008) emphasized that deformed trading time should primarily be understood as a mathematical convenience rather than as a directly observable variable, it may nevertheless be interpreted in reduced-form economic terms as capturing variation in the intensity of market activity over time. From this perspective, periods of accelerated trading time may correspond to episodes of elevated information arrival, heavier trading activity, lower market liquidity, or sentiment-driven bursts of investor participation, whereas periods of compressed trading time may reflect calmer market conditions. This interpretation is consistent with earlier time-subordination models in finance, such as Clark (1973), where price changes evolve in an operational rather than purely chronological time, and with Ghysels and Jasiak (1995), who relate time deformation to observable market variables such as trading volume, past returns, and leverage effects. It is also broadly consistent with Calvet and Fisher's (2007) multifrequency framework, in which shocks of heterogeneous durations affect return dynamics through the volatility of news. Hence, the MMAR need not be interpreted as implying that z_t is directly measurable; rather, it can be understood as a parsimonious latent summary of the changing intensity with which information, liquidity conditions, and investor sentiment are transmitted into asset prices.

From an applied perspective, the present findings may also have implications for both risk management and financial stability monitoring. If discontinuity and persistence in returns are governed by common MMAR-type mechanisms across otherwise unrelated asset markets, then extreme risk may not be viewed solely as an isolated feature of a single market or asset class. For financial institutions, this suggests that stress-testing frameworks and tail-risk models could be improved by accounting more explicitly for persistent and scale-invariant heavy-tail behavior across markets.

[12] Interestingly, Mandelbrot's (2008) also stresses that natural resources such as gold exhibit a clustering that conforms with binominal bending with probability $p = 0.60$.

From a regulatory perspective, the evidence of a common herding mechanism across equities, foreign exchange, commodities, and cryptocurrencies may indicate that episodes of market instability have a broader systemic component. In turn, this suggests that macroprudential and cross-sectoral monitoring of financial markets may be useful for identifying the build-up of common nonlinear risk patterns across different segments of the financial system.

5.3 Limitations

This study extended the recent study of Grobys (2023) by deriving simulation-based evidence for MMAR predictions concerning power-law behavior and persistence of financial asset returns. In doing so, we examined MMAR predictions for weekly and monthly data. The rationale for this choice is straightforward: Whereas monthly data is perhaps the most common frequency studied in asset pricing investigations concerned with equity markets, the literature on cryptocurrencies typically uses weekly data due to data availability (e.g., Liu et al., 2020, 2022; Shen et al., 2020). It is of course possible to extend the frequency to either higher or lower frequented data. There is, however, a problem arising from high-frequented data because Mandelbrot (2008) highlights that high frequency data may suffer from microstructure issues. Referring to Mandelbrot's (2008) notion on microstructure issues, Grobys (2023, p. 27) points out that "… foreign exchange rate data having a higher frequency than two hours or a lower frequency that 180 days are subject to crossovers: points where the mathematical relation takes a hold." Also, Mandelbrot (2008) highlights that crossovers are common for real as opposed to theoretical fractal data. Future research could extend the present study's framework to explore other data frequencies.[13] Furthermore, we tested the MMAR using weekly return data on five financial asset markets. Future research could employ our joint test to examine a larger variety of financial assets returns. This is, however, beyond the scope of the present research and therefore left for future studies.

A related question is why the present study focuses on the MMAR rather than on other long-memory or multifractal frameworks. The main reason is that the purpose of this paper is not only to examine persistence, but to study jointly the two characteristic traits emphasized by Mandelbrot (2008), namely discontinuity through power-law behavior and persistence through the Hurst exponent. Standard GARCH-type models and their long-memory extensions, such as FIGARCH, are primarily designed to capture persistence in conditional volatility dynamics, whereas the MMAR offers a natural framework in which scaling behavior, discontinuity, and persistence can be examined jointly through multifractal time deformation (Baillie et al., 1996; Bollerslev and Mikkelsen, 1996; Mandelbrot et al., 1997). Other multifractal approaches, such as the Markov-switching multifractal model of Calvet and Fisher (2004), also provide important alternatives. However, the MMAR is especially relevant in the present setting because it is the original framework linking Mandelbrot's notion of deformed trading time to the joint behavior of tails and persistence in asset returns. In

[13] Note that Hou et al. (2020) call for scientific replications for documented research. The authors argue that this is an important issue due to the high rate of replication failure in financial economics and because financial economics as a discipline is observational in its nature.

this sense, the choice of MMAR reflects the specific theoretical focus of the present study rather than any claim that competing models are not useful.

Another issue is the choice of the binominal-bending parameters $p \in \{0.55, 0.60, \ldots, 0.85\}$ used to generate the multiplicative cascades. The purpose of this range is to cover a broad spectrum of time deformation from relatively mild to relatively wild trading-time dynamics. Intuitively, lower values of p imply less concentrated binomial branching and therefore milder return behavior, whereas higher values of p imply more concentrated branching and hence stronger time deformation, more pronounced discontinuity, and greater persistence. This parameter range also follows Grobys (2023), who uses the same grid in a related multifractal setting. In the present study, the simulation results indicate that this range is sufficiently broad: for lower values of p, the expected power-law exponents imply comparatively mild tail behavior, whereas for higher values of p, the expected exponents become small enough to imply very wild return dynamics with undefined low-order moments. Thus, the selected parameter range is designed to capture the transition from mild to wild MMAR behavior within a transparent and systematic simulation framework.

6 Conclusion

Extending earlier research on the MMAR, this study provides simulation-based evidence for predicted power-law behavior and persistence of financial asset returns. Empirical asset pricing research proposed an abundance of factor models in attempts to explain the return evolutions of financial assets—a phenomenon that Feng et al. (2020) dubbed a "factor zoo." However, these factor models do not tell us anything about the two key traits of financial assets—discontinuity and price persistence (Mandelbrot, 2008). It is a well-established fact that power-law behavior is a universal feature of the returns on financial assets (Lux and Alfarano, 2016). Segnon and Lux (2013) stressed that multifractal measures have been adapted to asset-price modeling and are designed to generate data exhibiting the two key traits of financial asset returns.

Despite of its appealing features, the literature on empirical tests of the original MMAR is rare. This study is the first that documents simulation-based evidence for predicted power-law behavior and price persistence produced by the MMAR. Using the estimated joint distributions of power-law exponents and Hurst exponents derived from our MMAR simulations, we propose a new joint test that is designed to test whether the MMAR is capable of explaining the two key traits of financial asset returns. Remarkably, the evidence suggests that the benchmark MMAR specification employed here is capable of describing the power-law behavior and price persistence observed across otherwise unrelated asset market, including Bitcoin. Because power-law behavior in the returns on financial assets has been associated with herding behavior (Lux, 1995; Lux & Marchesi, 1999), our findings are consistent with the possibility that common latent mechanisms, including herding, may contribute to return dynamics across otherwise unrelated asset markets. At the same time, the present study does not provide direct behavioral evidence on herding, and other mechanisms such as liquidity conditions, information arrival, or investor sentiment may also play a role.

Appendix 1

Table 11 Descriptive statistics of various financial assets

Panel A. Descriptive statistics for weekly data					
	SP500	USD/GPB	Gold futures	Crude oil futures	Bitcoin
Mean	0.002555	0.000299	0.002131	0.003016	0.016328
Median	0.004200	0.000000	0.002150	0.006000	0.007450
Maximum	0.121000	0.062800	0.111600	0.317500	0.436200
Minimum	-0.149800	-0.065400	-0.093400	-0.293100	-0.416900
Std. Dev	0.023912	0.013150	0.020213	0.057842	0.103173
Skewness	-0.645866	0.402213	0.218583	0.121984	0.287480
Kurtosis	9.668048	6.194273	6.146813	8.195470	5.026978
Jarque–Bera (JB test)	876.4973	206.1592	191.7774	513.9962	84.34512
p-value JB test	0.000000	0.000000	0.000000	0.000000	0.000000
Observations	456	456	456	456	456
Panel B. Descriptive statistics for monthly data					
	SP500	USD/GPB	Gold futures	Crude oil futures	
Mean	0.754456	0.058028	0.442211	0.193887	
Median	1.203600	0.111450	-0.013006	0.786048	
Maximum	12.37801	13.05875	16.31516	63.32687	
Minimum	-24.54280	-13.59389	-20.13356	-78.18661	
Std. Dev	4.377792	2.802532	4.614615	10.40905	
Skewness	-0.872618	0.187489	0.020455	-0.437500	
Kurtosis	5.882993	5.374110	4.243620	12.37052	
Jarque–Bera (JB test)	247.4633	125.0185	33.196911	1929.687	
p-value JB test	0.000000	0.000000	0.000000	0.000000	
Observations	534	534	534	534	

Panel A reports descriptive statistics for weekly log-return data on the U.S. S&P 500, USD/GBP exchange rate, gold futures (Dec 24 (GCZ4)), crude oil futures (Nov 24 (CLX4)), and Bitcoin. Due to data availability on Bitcoin, the weekly sample runs from January 3, 2016 to September 22, 2024, comprising 456 observations. Panel B reports descriptive statistics for monthly log-return data on the U.S. S&P 500, USD/GBP exchange rate, gold futures, and crude oil futures. The monthly sample runs from October 1981 to March 2026, comprising 534 observations.

Table 12 Monthly multifractal return data derived from a multiplicative cascade with binominal bending and $p = 0.55$

Distribution	MAX	MIN	Mean	VAR	$\ddot{\alpha}$	$\ddot{x}_{min}$	% #PL state	*p*-value GoF	MAX #t in PL state	$\ddot{H}$
<2.5%	11.92	-24.29	-0.66	22.15	2.87	3.64	0.05	0.00	1	0.44
<5%	12.55	-22.71	-0.55	22.90	3.08	4.12	0.06	0.00	2	0.46
Median	16.43	-16.22	0.02	26.96	4.46	6.80	0.19	0.27	3	0.56
>95%	23.18	-12.55	0.55	31.62	7.39	10.11	0.41	0.92	7	0.66
>97.5%	24.73	-12.05	0.64	32.66	8.54	10.95	0.47	0.96	8	0.67
Min	9.56	-34.03	-1.02	18.71	2.37	2.55	0.03	0.00	1	0.37
Max	32.23	-9.97	1.12	35.71	17.45	12.93	0.58	1.00	13	0.77
Mean	16.96	-16.81	0.01	27.05	4.78	6.94	0.21	0.36	3.68	0.56
Std.Dev	3.38	3.21	0.33	2.69	1.49	1.88	0.11	0.32	1.71	0.06

This Table reports the distribution of the maxima, minima, means, variances, estimated power-law exponent,$\ddot{\alpha}$, estimated cutoffs,$\ddot{x}_{min}$, percentage of observations governed by a power law with parametrization ($\ddot{\alpha}$,$\ddot{x}_{min}$), *p*-values of Clauset et al.'s (2009) goodness-of-fit tests, the maximum time lengths in power-law regimes measured in terms of consecutive observations, and the estimated Hurst exponents,$\ddot{H}$. The multifractal return data is based on a monthly frequency (512 observations), and derived from a multiplicative cascade with binominal bending with$p = 0.55$

Table 13 Monthly multifractal return data derived from a multiplicative cascade with binominal bending and$p = 0.60$

Distribution	MAX	MIN	Mean	VAR	$\ddot{\alpha}$	$\ddot{x}_{min}$	% #PL state	*p*-value GoF	MAX #t in PL state	$\ddot{H}$
<2.5%	17.07	-49.36	-0.87	34.39	2.47	3.37	0.06	0.00	2	0.45
<5%	18.06	-43.68	-0.69	35.55	2.58	3.86	0.07	0.00	2	0.47
Median	26.05	-25.94	0.01	44.03	3.49	7.41	0.21	0.32	4	0.57
>95%	45.05	-18.13	0.71	56.17	5.47	12.99	0.45	0.92	10	0.67
>97.5%	50.90	-17.15	0.84	59.08	6.16	14.00	0.50	0.96	10	0.69
Min	13.62	-77.01	-1.24	29.22	2.13	2.27	0.03	0.00	1	0.38
Max	73.12	-14.23	1.57	69.25	9.17	17.39	0.64	1.00	17	0.79
Mean	28.01	-27.65	0.01	44.80	3.68	7.72	0.23	0.37	4.79	0.57
Std.Dev	8.60	8.07	0.43	6.36	0.98	2.81	0.12	0.32	2.30	0.06

This Table reports the distribution of the maxima, minima, means, variances, estimated power-law exponent,$\ddot{\alpha}$, estimated cutoffs,$\ddot{x}_{min}$, percentage of observations governed by a power law with parametrization ($\ddot{\alpha}$,$\ddot{x}_{min}$), *p*-values of Clauset et al.'s (2009) goodness-of-fit tests, the maximum time lengths in power-law regimes measured in terms of consecutive observations, and the estimated Hurst exponents,$\ddot{H}$. The multifractal return data is based on a monthly frequency (512 observations), and derived from a multiplicative cascade with binominal bending with$p = 0.60$

Table 14 Monthly multifractal return data derived from a multiplicative cascade with binominal bending and $p = 0.65$

Distribution	MAX	MIN	Mean	VAR	$\ddot{\alpha}$	$\ddot{x}_{min}$	% #PL state	p-value GoF	MAX #t in PL state	$\ddot{H}$
<2.5%	24.97	-106.09	-1.20	60.09	2.09	2.83	0.06	0.00	2	0.47
<5%	27.30	-93.34	-0.92	63.35	2.18	3.35	0.08	0.00	2	0.49
Median	45.30	-44.59	0.03	85.50	2.86	8.05	0.23	0.28	5	0.60
>95%	90.48	-27.75	0.99	128.59	4.23	16.49	0.50	0.91	12	0.71
>97.5%	108.89	-25.67	1.17	144.52	4.73	18.29	0.53	0.97	15	0.72
Min	16.93	-167.18	-1.78	49.85	1.83	1.40	0.04	0.00	1	0.42
Max	172.61	-19.23	2.25	202.40	8.12	27.58	0.74	1.00	27	0.81
Mean	50.24	-49.39	0.02	89.46	2.98	8.79	0.25	0.35	6.06	0.59
Std.Dev	20.92	19.79	0.60	21.06	0.67	4.21	0.13	0.31	3.25	0.07

This Table reports the distribution of the maxima, minima, means, variances, estimated power-law exponent, $\ddot{\alpha}$, estimated cutoffs, $\ddot{x}_{min}$, percentage of observations governed by a power law with parametrization ($\ddot{\alpha}$, $\ddot{x}_{min}$), p-values of Clauset et al.'s (2009) goodness-of-fit tests, the maximum time lengths in power-law regimes measured in terms of consecutive observations, and the estimated Hurst exponents, $\ddot{H}$. The multifractal return data is based on a monthly frequency (512 observations), and derived from a multiplicative cascade with binominal bending with $p = 0.65$

Table 15 Monthly multifractal return data derived from a multiplicative cascade with binominal bending and $p = 0.70$

Distribution	MAX	MIN	Mean	VAR	$\ddot{\alpha}$	$\ddot{x}_{min}$	% #PL state	p-value GoF	MAX #t in PL state	$\ddot{H}$
<2.5%	37.80	-230.88	-1.78	113.23	1.87	2.29	0.06	0.00	2	0.49
<5%	42.28	-194.07	-1.48	123.11	1.93	2.66	0.07	0.00	3	0.51
Median	79.70	-78.46	0.03	189.19	2.44	8.42	0.24	0.25	6	0.62
>95%	192.51	-42.83	1.49	378.95	3.60	23.36	0.52	0.93	14	0.74
>97.5%	231.03	-37.79	1.83	440.80	4.01	27.36	0.56	0.97	17	0.76
Min	25.59	-351.47	-3.06	86.07	1.67	1.20	0.03	0.00	1	0.44
Max	385.52	-26.86	3.22	760.30	5.67	42.17	0.73	1.00	27	0.84
Mean	92.55	-90.61	0.03	210.56	2.56	10.00	0.26	0.35	7.02	0.62
Std.Dev	49.20	47.12	0.91	83.50	0.56	6.49	0.14	0.32	3.87	0.07

This Table reports the distribution of the maxima, minima, means, variances, estimated power-law exponent, $\ddot{\alpha}$, estimated cutoffs, $\ddot{x}_{min}$, percentage of observations governed by a power law with parametrization ($\ddot{\alpha}$, $\ddot{x}_{min}$), p-values of Clauset et al.'s (2009) goodness-of-fit tests, the maximum time lengths in power-law regimes measured in terms of consecutive observations, and the estimated Hurst exponents, $\ddot{H}$. The multifractal return data is based on a monthly frequency (512 observations), and derived from a multiplicative cascade with binominal bending with $p = 0.70$

Table 16 Monthly multifractal return data derived from a multiplicative cascade with binominal bending and$p = 0.75$

Distribution	MAX	MIN	Mean	VAR	$\ddot{\alpha}$	$\ddot{x}_{min}$	% #PL state	p-value GoF	MAX #t in PL state	$\ddot{H}$
<2.5%	55.34	-468.50	-2.83	211.44	1.70	1.58	0.05	0.00	2	0.52
<5%	62.71	-401.81	-2.32	242.37	1.75	2.20	0.07	0.00	3	0.54
Median	137.31	-135.79	0.04	466.14	2.17	8.38	0.24	0.25	7	0.66
>95%	407.09	-63.47	2.44	1264.62	3.07	29.37	0.51	0.93	18	0.78
>97.5%	482.78	-55.61	2.90	1506.46	3.30	36.69	0.59	0.97	21	0.80
Min	38.84	-720.11	-5.33	130.53	1.50	0.48	0.03	0.00	1	0.41
Max	822.76	-34.70	4.76	3010.29	5.38	50.97	0.84	1.00	47	0.87
Mean	171.16	-168.37	0.04	568.03	2.24	10.95	0.27	0.35	7.97	0.66
Std.Dev	112.17	107.21	1.47	352.83	0.43	8.86	0.14	0.32	4.81	0.07

This Table reports the distribution of the maxima, minima, means, variances, estimated power-law exponent,$\ddot{\alpha}$, estimated cutoffs,$\ddot{x}_{min}$, percentage of observations governed by a power law with parametrization ($\ddot{\alpha}$,$\ddot{x}_{min}$), p-values of Clauset et al.'s (2009) goodness-of-fit tests, the maximum time lengths in power-law regimes measured in terms of consecutive observations, and the estimated Hurst exponents,$\ddot{H}$. The multifractal return data is based on a monthly frequency (512 observations), and derived from a multiplicative cascade with binominal bending with$p = 0.75$

Table 17 Monthly multifractal return data derived from a multiplicative cascade with binominal bending and $p = 0.80$

Distribution	MAX	MIN	Mean	VAR	$\ddot{\alpha}$	$\ddot{x}_{min}$	% #PL state	p-value GoF	MAX #t in PL state	$\ddot{H}$
<2.5%	78.21	-995.19	-4.82	411.75	1.58	1.14	0.05	0.00	2	0.55
<5%	88.61	-794.46	-4.09	491.96	1.62	1.43	0.07	0.00	3	0.57
Median	230.24	-230.07	0.04	1195.16	1.96	7.81	0.24	0.28	7	0.70
>95%	847.65	-88.56	4.41	4423.64	2.72	38.19	0.52	0.93	18	0.83
>97.5%	983.62	-77.10	5.15	6127.11	2.95	47.09	0.57	0.96	23	0.85
Min	48.40	-1532.36	-8.98	197.64	1.50	0.57	0.04	0.00	2	0.45
Max	1782.86	-43.47	7.35	13,140.99	4.28	79.51	0.70	1.00	46	0.93
Mean	312.94	-310.92	0.06	1704.21	2.03	11.85	0.26	0.35	8.73	0.70
Std.Dev	248.78	236.76	2.53	1499.79	0.35	12.00	0.14	0.31	5.56	0.08

This Table reports the distribution of the maxima, minima, means, variances, estimated power-law exponent, $\ddot{\alpha}$, estimated cutoffs, $\ddot{x}_{min}$, percentage of observations governed by a power law with parametrization ($\ddot{\alpha}$, $\ddot{x}_{min}$), p-values of Clauset et al.'s (2009) goodness-of-fit tests, the maximum time lengths in power-law regimes measured in terms of consecutive observations, and the estimated Hurst exponents, $\ddot{H}$. The multifractal return data is based on a monthly frequency (512 observations), and derived from a multiplicative cascade with binominal bending with $p = 0.80$

Table 18 Monthly multifractal return data derived from a multiplicative cascade with binominal bending and$p = 0.85$

Distribution	MAX	MIN	Mean	VAR	$\ddot{\alpha}$	$\ddot{x}_{min}$	% #PL state	*p*-value GoF	MAX #t in PL state	$\ddot{H}$
<2.5%	96.80	-1954.91	-8.60	773.75	1.47	0.58	0.06	0.00	2	0.59
<5%	130.88	-1607.86	-7.52	916.27	1.50	0.66	0.07	0.00	3	0.61
Median	353.10	-353.90	-0.10	3386.16	1.77	5.10	0.26	0.22	9	0.74
>95%	1708.15	-130.74	7.93	16,128.96	2.40	38.81	0.55	0.92	19	0.87
>97.5%	1956.78	-98.13	9.39	24,254.37	2.50	46.64	0.57	0.96	23	0.89
Min	54.98	-3255.20	-14.75	287.38	1.39	0.17	0.03	0.00	2	0.48
Max	3705.71	-48.96	13.98	55,056.02	4.23	86.52	0.78	1.00	37	0.96
Mean	567.41	-565.66	0.08	5530.60	1.84	10.68	0.27	0.33	9.47	0.74
Std.Dev	537.39	511.25	4.57	6239.61	0.28	13.07	0.14	0.32	5.83	0.08

This Table reports the distribution of the maxima, minima, means, variances, estimated power-law exponent,$\ddot{\alpha}$, estimated cutoffs,$\ddot{x}_{min}$, percentage of observations governed by a power law with parametrization ($\ddot{\alpha}$,$\ddot{x}_{min}$), *p*-values of Clauset et al.'s (2009) goodness-of-fit tests, the maximum time lengths in power-law regimes measured in terms of consecutive observations, and the estimated Hurst exponents,$\ddot{H}$. The multifractal return data is based on a monthly frequency (512 observations), and derived from a multiplicative cascade with binominal bending with$p = 0.85$

Table 19 Weekly multifractal return data derived from a multiplicative cascade with binominal bending and$p = 0.55$and subsample 1

Distribution	MAX	MIN	Mean	VAR	$\ddot{\alpha}$	$\ddot{x}_{min}$	% #PL state	p-value GoF	MAX #t in PL state	$\ddot{H}$
<2.5%	7.56	-15.34	-0.26	7.07	3.11	2.37	0.04	0.00	1	0.46
<5%	7.88	-14.48	-0.21	7.21	3.32	2.61	0.04	0.00	2	0.47
Median	10.29	-10.01	0.00	8.12	4.71	4.18	0.14	0.24	3	0.54
>95%	13.99	-7.92	0.22	9.14	7.78	6.18	0.33	0.90	7	0.62
>97.5%	14.86	-7.61	0.25	9.34	9.03	6.45	0.38	0.95	8	0.64
Min	6.59	-19.64	0.04	6.24	2.64	1.73	0.02	0.00	1	0.40
Max	22.26	-6.54	0.41	10.08	13.49	7.38	0.52	1.00	12	0.69
Mean	10.45	-10.42	0.00	8.13	5.06	4.26	0.16	0.34	3.66	0.55
Std.Dev	1.94	1.99	0.13	0.58	1.50	1.08	0.09	0.31	1.62	0.05

Weekly data obtained from the MMAR is split into two non-overlapping subsamples of equal length. This Table reports the distribution of the maxima, minima, means, variances, estimated power-law exponent,$\ddot{\alpha}$, estimated cutoffs,$\ddot{x}_{min}$, percentage of observations governed by a power law with parametrization ($\ddot{\alpha}$,$\ddot{x}_{min}$), p-values of Clauset et al.'s (2009) goodness-of-fit tests, the maximum time lengths in power-law regimes measured in terms of consecutive observations, and the estimated Hurst exponents,$\ddot{H}$for the first subsample (512 observations). Data are derived from a multiplicative cascade with binominal bending with$p = 0.55$

Table 20 Weekly multifractal return data derived from a multiplicative cascade with binominal bending with$p = 0.55$and subsample 2

Distribution	MAX	MIN	Mean	VAR	$\ddot{\alpha}$	$\ddot{x}_{min}$	% #PL state	p-value GoF	MAX #t in PL state	$\ddot{H}$
<2.5%	6.30	-12.21	-0.19	4.70	3.19	2.02	0.04	0.00	2	0.45
<5%	6.53	-11.07	-0.16	4.78	3.38	2.18	0.05	0.00	2	0.47
Median	8.32	-8.22	0.00	5.41	4.83	3.48	0.13	0.25	3	0.55
>95%	11.57	-6.41	0.16	6.09	7.51	5.03	0.32	0.91	7	0.62
>97.5%	12.31	-6.11	0.20	6.22	8.21	5.30	0.36	0.96	8	0.64
Min	5.72	-16.34	-0.29	4.09	2.50	1.20	0.02	0.00	1	0.41
Max	17.46	-5.43	0.32	6.60	13.52	5.90	0.59	1.00	14	0.70
Mean	8.57	-10.42	0.00	8.13	5.06	4.26	0.16	0.34	3.66	0.55
Std.Dev	1.57	1.99	0.13	0.58	1.50	1.08	0.09	0.31	1.62	0.05

Weekly data obtained from the MMAR is split into two non-overlapping subsamples of equal length. This Table reports the distribution of the maxima, minima, means, variances, estimated power-law exponent,$\ddot{\alpha}$, estimated cutoffs,$\ddot{x}_{min}$, percentage of observations governed by a power law with parametrization ($\ddot{\alpha}$,$\ddot{x}_{min}$), p-values of Clauset et al.'s (2009) goodness-of-fit tests, the maximum time lengths in power-law regimes measured in terms of consecutive observations, and the estimated Hurst exponents,$\ddot{H}$for the second subsample (512 observations). Data are derived from a multiplicative cascade with binominal bending with$p = 0.55$

Table 21 Weekly multifractal return data derived from a multiplicative cascade with binominal bending and$p = 0.60$and subsample 1

Distribution	MAX	MIN	Mean	VAR	$\ddot{\alpha}$	$\ddot{x}_{min}$	% #PL state	p-value GoF	MAX #t in PL state	$\ddot{H}$
<2.5%	12.28	-35.84	-0.36	12.61	2.56	2.34	0.04	0.00	2	0.47
<5%	13.01	-31.65	-0.29	12.97	2.68	2.63	0.05	0.00	2	0.48
Median	18.15	-18.38	0.01	15.42	3.57	4.89	0.16	0.23	5	0.56
>95%	30.87	-13.09	0.30	18.53	5.36	8.53	0.37	0.92	10	0.64
>97.5%	34.73	-12.18	0.35	19.29	5.87	9.25	0.43	0.98	11	0.66
Min	9.93	-50.68	-0.56	11.19	2.26	1.78	0.02	0.00	1	0.41
Max	59.46	-10.62	0.51	22.76	10.48	11.77	0.51	1.00	21	0.71
Mean	19.48	-19.81	0.01	15.55	3.73	5.15	0.18	0.33	5.13	0.56
Std.Dev	5.75	5.99	0.18	1.70	0.89	1.81	0.10	0.32	2.41	0.05

Weekly data obtained from the MMAR is split into two non-overlapping subsamples of equal length. This Table reports the distribution of the maxima, minima, means, variances, estimated power-law exponent,$\ddot{\alpha}$, estimated cutoffs,$\ddot{x}_{min}$, percentage of observations governed by a power law with parametrization ($\ddot{\alpha}$,$\ddot{x}_{min}$), p-values of Clauset et al.'s (2009) goodness-of-fit tests, the maximum time lengths in power-law regimes measured in terms of consecutive observations, and the estimated Hurst exponents,$\ddot{H}$for the first subsample (512 observations). Data are derived from a multiplicative cascade with binominal bending with$p = 0.60$

Table 22 Weekly multifractal return data derived from a multiplicative cascade with binominal bending and$p = 0.60$and subsample 2

Distribution	MAX	MIN	Mean	VAR	$\ddot{\alpha}$	$\ddot{x}_{min}$	% #PL state	p-value GoF	MAX #t in PL state	$\ddot{H}$
<2.5%	8.26	-21.91	-0.21	5.67	2.60	1.64	0.04	0.00	2	0.47
<5%	8.89	-19.64	-0.17	5.82	2.69	1.75	0.05	0.00	2	0.49
Median	12.48	-12.27	0.00	6.84	3.60	3.31	0.16	0.27	4	0.57
>95%	20.41	-8.80	0.18	8.15	5.51	5.73	0.37	0.91	9	0.65
>97.5%	23.07	-8.22	0.23	8.42	6.15	6.46	0.40	0.95	11	0.67
Min	6.87	-36.44	-0.30	4.47	2.32	1.14	0.02	0.00	1	0.41
Max	29.92	-6.96	0.36	9.68	8.61	8.78	0.54	1.00	24	0.73
Mean	13.29	-13.01	0.00	6.89	3.77	3.50	0.18	0.34	4.93	0.57
Std.Dev	3.67	3.44	0.11	0.72	0.88	1.24	0.10	0.31	2.36	0.05

Weekly data obtained from the MMAR is split into two non-overlapping subsamples of equal length. This Table reports the distribution of the maxima, minima, means, variances, estimated power-law exponent,$\ddot{\alpha}$, estimated cutoffs,$\ddot{x}_{min}$, percentage of observations governed by a power law with parametrization ($\ddot{\alpha}$,$\ddot{x}_{min}$), p-values of Clauset et al.'s (2009) goodness-of-fit tests, the maximum time lengths in power-law regimes measured in terms of consecutive observations, and the estimated Hurst exponents,$\ddot{H}$for the second subsample (512 observations). Data are derived from a multiplicative cascade with binominal bending with$p = 0.60$

Table 23 Weekly multifractal return data derived from a multiplicative cascade with binominal bending and$p = 0.65$and subsample 1

Distribution	MAX	MIN	Mean	VAR	$\ddot{\alpha}$	$\ddot{x}_{min}$	% #PL state	p-value GoF	MAX #t in PL state	$\ddot{H}$
<2.5%	20.40	-88.58	-0.53	24.74	2.19	2.18	0.04	0.00	2	0.48
<5%	22.17	-71.33	-0.44	26.04	2.27	2.52	0.05	0.00	2	0.50
Median	34.59	-35.43	0.01	33.50	2.88	5.60	0.18	0.21	6	0.59
>95%	68.22	-22.91	0.48	47.40	4.20	12.13	0.39	0.91	12	0.67
>97.5%	86.37	-21.16	0.53	51.78	4.53	13.41	0.45	0.96	14	0.69
Min	15.56	-126.03	-0.87	20.81	1.99	1.45	0.02	0.00	1	0.43
Max	154.20	-16.85	0.79	77.29	5.99	19.56	0.56	1.00	26	0.74
Mean	38.61	-39.55	0.01	34.73	3.00	6.30	0.19	0.32	6.51	0.59
Std.Dev	16.07	16.34	0.27	6.92	0.60	3.02	0.11	0.31	3.33	0.05

Weekly data obtained from the MMAR is split into two non-overlapping subsamples of equal length. This Table reports the distribution of the maxima, minima, means, variances, estimated power-law exponent,$\ddot{\alpha}$, estimated cutoffs,$\ddot{x}_{min}$, percentage of observations governed by a power law with parametrization ($\ddot{\alpha}$,$\ddot{x}_{min}$), p-values of Clauset et al.'s (2009) goodness-of-fit tests, the maximum time lengths in power-law regimes measured in terms of consecutive observations, and the estimated Hurst exponents,$\ddot{H}$for the first subsample (512 observations). Data are derived from a multiplicative cascade with binominal bending with$p = 0.65$

Table 24 Weekly multifractal return data derived from a multiplicative cascade with binominal bending and$p = 0.65$and subsample 2

Distribution	MAX	MIN	Mean	VAR	$\ddot{\alpha}$	$\ddot{x}_{min}$	% #PL state	p-value GoF	MAX #t in PL state	$\ddot{H}$
<2.5%	11.39	-41.00	-0.25	7.19	2.21	1.22	0.04	0.00	2	0.49
<5%	12.43	-36.00	-0.21	7.59	2.29	1.38	0.05	0.00	3	0.51
Median	19.25	-19.44	0.00	9.78	2.86	3.02	0.18	0.23	6	0.60
>95%	37.89	-12.31	0.22	13.36	4.12	6.54	0.39	0.91	12	0.70
>97.5%	42.64	-11.33	0.27	14.27	4.39	7.23	0.44	0.96	14	0.72
Min	8.04	-75.63	-0.39	5.44	2.02	0.88	0.02	0.00	1	0.43
Max	58.88	-8.57	0.45	18.63	7.46	11.06	0.55	1.00	22	0.79
Mean	21.44	-21.05	0.00	10.05	3.00	3.40	0.19	0.33	6.34	0.60
Std.Dev	8.09	7.68	0.13	1.81	0.61	1.63	0.11	0.32	3.09	0.06

Weekly data obtained from the MMAR is split into two non-overlapping subsamples of equal length. This Table reports the distribution of the maxima, minima, means, variances, estimated power-law exponent,$\ddot{\alpha}$, estimated cutoffs,$\ddot{x}_{min}$, percentage of observations governed by a power law with parametrization ($\ddot{\alpha}$,$\ddot{x}_{min}$), p-values of Clauset et al.'s (2009) goodness-of-fit tests, the maximum time lengths in power-law regimes measured in terms of consecutive observations, and the estimated Hurst exponents,$\ddot{H}$for the second subsample (512 observations). Data are derived from a multiplicative cascade with binominal bending with$p = 0.65$

Table 25 Weekly multifractal return data derived from a multiplicative cascade with binominal bending and$p = 0.70$and subsample 1

Distribution	MAX	MIN	Mean	VAR	$\ddot{\alpha}$	$\ddot{x}_{min}$	% #PL state	p-value GoF	MAX #t in PL state	$\ddot{H}$
<2.5%	32.53	-202.05	-0.80	51.72	1.94	1.94	0.04	0.00	2	0.51
<5%	36.12	-158.57	-0.65	55.54	2.01	2.31	0.05	0.00	3	0.53
Median	66.42	-68.17	0.01	80.68	2.43	5.82	0.20	0.19	7	0.62
>95%	156.42	-38.97	0.72	153.43	3.41	16.83	0.41	0.91	17	0.71
>97.5%	199.24	-36.33	0.86	180.75	3.69	19.42	0.45	0.95	19	0.72
Min	22.98	-308.55	-1.61	40.53	1.65	0.60	0.02	0.00	2	0.43
Max	372.40	-25.45	1.37	341.19	5.47	31.52	0.76	1.00	31	0.77
Mean	77.11	-78.82	0.02	88.92	2.53	7.32	0.21	0.31	7.87	0.62
Std.Dev	41.46	41.34	0.42	32.62	0.46	4.75	0.11	0.31	4.41	0.05

Weekly data obtained from the MMAR is split into two non-overlapping subsamples of equal length. This Table reports the distribution of the maxima, minima, means, variances, estimated power-law exponent,$\ddot{\alpha}$, estimated cutoffs,$\ddot{x}_{min}$, percentage of observations governed by a power law with parametrization ($\ddot{\alpha}$,$\ddot{x}_{min}$), p-values of Clauset et al.'s (2009) goodness-of-fit tests, the maximum time lengths in power-law regimes measured in terms of consecutive observations, and the estimated Hurst exponents,$\ddot{H}$for the first subsample (512 observations). Data are derived from a multiplicative cascade with binominal bending with$p = 0.70$

Table 26 Weekly multifractal return data derived from a multiplicative cascade with binominal bending and $p = 0.70$ and subsample 2

Distribution	MAX	MIN	Mean	VAR	$\ddot{\alpha}$	$\ddot{x}_{min}$	% #PL state	p-value GoF	MAX #t in PL state	$\ddot{H}$
<2.5%	14.94	-76.38	-0.33	9.58	1.94	0.83	0.04	0.00	3	0.53
<5%	16.09	-66.70	-0.28	10.12	1.99	0.93	0.06	0.00	3	0.54
Median	29.94	-29.85	0.00	15.50	2.46	2.68	0.18	0.19	7	0.65
>95%	70.48	-16.21	0.28	26.57	3.30	7.14	0.42	0.93	15	0.76
>97.5%	82.14	-14.89	0.36	29.76	3.63	8.49	0.45	0.97	18	0.78
Min	10.21	-145.18	-0.50	7.14	1.79	0.48	0.02	0.00	2	0.45
Max	116.25	-10.52	0.57	52.32	4.91	12.52	0.58	1.00	24	0.87
Mean	34.23	-33.77	0.00	16.39	2.54	3.19	0.20	0.32	7.53	0.65
Std.Dev	16.69	16.07	0.17	5.20	0.45	2.02	0.11	0.32	3.74	0.07

Weekly data obtained from the MMAR is split into two non-overlapping subsamples of equal length. This Table reports the distribution of the maxima, minima, means, variances, estimated power-law exponent, $\ddot{\alpha}$, estimated cutoffs, $\ddot{x}_{min}$, percentage of observations governed by a power law with parametrization ($\ddot{\alpha}$, $\ddot{x}_{min}$), p-values of Clauset et al.'s (2009) goodness-of-fit tests, the maximum time lengths in power-law regimes measured in terms of consecutive observations, and the estimated Hurst exponents, $\ddot{H}$ for the second subsample (512 observations). Data are derived from a multiplicative cascade with binominal bending with $p = 0.70$

Table 27 Weekly multifractal return data derived from a multiplicative cascade with binominal bending and $p = 0.75$ and subsample 1

Distribution	MAX	MIN	Mean	VAR	$\ddot{\alpha}$	$\ddot{x}_{min}$	% #PL state	p-value GoF	MAX #t in PL state	$\ddot{H}$
<2.5%	50.60	-442.91	-1.29	106.98	1.77	1.54	0.04	0.00	2	0.54
<5%	57.61	-364.61	-1.05	120.37	1.81	1.81	0.05	0.00	3	0.56
Median	123.28	-125.43	0.01	205.09	2.15	6.04	0.20	0.17	8	0.66
>95%	356.98	-62.14	1.20	552.42	2.94	22.57	0.41	0.91	18	0.74
>97.5%	456.02	-56.72	1.53	692.93	3.12	27.97	0.45	0.96	22	0.77
Min	37.26	-708.80	-2.84	80.99	1.65	0.83	0.03	0.00	2	0.47
Max	845.71	-38.13	2.30	1561.33	3.83	43.35	0.60	1.00	34	0.81
Mean	151.45	-154.06	0.02	254.54	2.22	8.16	0.21	0.30	9.02	0.65
Std.Dev	100.24	98.41	0.70	154.96	0.35	6.73	0.11	0.31	5.15	0.06

Weekly data obtained from the MMAR is split into two non-overlapping subsamples of equal length. This Table reports the distribution of the maxima, minima, means, variances, estimated power-law exponent, $\ddot{\alpha}$, estimated cutoffs, $\ddot{x}_{min}$, percentage of observations governed by a power law with parametrization ($\ddot{\alpha}$, $\ddot{x}_{min}$), p-values of Clauset et al.'s (2009) goodness-of-fit tests, the maximum time lengths in power-law regimes measured in terms of consecutive observations, and the estimated Hurst exponents, $\ddot{H}$ for the first subsample (512 observations). Data are derived from a multiplicative cascade with binominal bending with $p = 0.75$

Table 28 Weekly multifractal return data derived from a multiplicative cascade with binominal bending and$p = 0.75$and subsample 2

Distribution	MAX	MIN	Mean	VAR	$\ddot{\alpha}$	$\ddot{x}_{min}$	% #PL state	p-value GoF	MAX #t in PL state	$\ddot{H}$
<2.5%	17.55	-140.61	-0.46	12.25	1.76	0.47	0.04	0.00	3	0.56
<5%	19.89	-121.13	-0.38	13.25	1.80	0.57	0.05	0.00	3	0.58
Median	43.18	-43.68	0.00	24.78	2.19	2.32	0.17	0.22	8	0.70
>95%	123.11	-19.57	0.39	60.65	2.88	7.50	0.42	0.94	18	0.83
>97.5%	147.34	-17.01	0.45	67.31	3.15	9.07	0.46	0.96	22	0.85
Min	11.40	-257.44	-0.69	9.23	1.64	0.27	0.02	0.00	1	0.49
Max	211.26	-11.43	0.73	145.97	4.47	14.26	0.58	1.00	43	0.94
Mean	52.83	-52.13	0.00	28.82	2.24	2.83	0.21	0.33	8.73	0.70
Std.Dev	32.16	31.21	0.23	15.07	0.37	2.25	0.12	0.32	4.97	0.07

Weekly data obtained from the MMAR is split into two non-overlapping subsamples of equal length. This Table reports the distribution of the maxima, minima, means, variances, estimated power-law exponent,$\ddot{\alpha}$, estimated cutoffs,$\ddot{x}_{min}$, percentage of observations governed by a power law with parametrization ($\ddot{\alpha}$,$\ddot{x}_{min}$), p-values of Clauset et al.'s (2009) goodness-of-fit tests, the maximum time lengths in power-law regimes measured in terms of consecutive observations, and the estimated Hurst exponents,$\ddot{H}$for the second subsample (512 observations). Data are derived from a multiplicative cascade with binominal bending with$p = 0.75$

Table 29 Weekly multifractal return data derived from a multiplicative cascade with binominal bending and$p = 0.80$and subsample 1

Distribution	MAX	MIN	Mean	VAR	$\ddot{\alpha}$	$\ddot{x}_{min}$	% #PL state	p-value GoF	MAX #t in PL state	$\ddot{H}$
<2.5%	72.54	-923.18	-2.35	221.16	1.63	1.03	0.04	0.00	2	0.57
<5%	87.06	-772.15	-1.94	256.78	1.65	1.23	0.04	0.00	3	0.59
Median	215.81	-215.74	-0.02	558.26	1.95	5.90	0.18	0.17	9	0.70
>95%	787.24	-96.83	2.16	2116.93	2.62	32.33	0.41	0.91	21	0.79
>97.5%	957.06	-81.90	2.64	2968.58	2.86	37.90	0.44	0.97	23	0.80
Min	47.47	-1540.69	-4.84	144.37	1.53	0.48	0.02	0.00	2	0.51
Max	1820.49	-53.36	3.63	6842.17	4.30	57.84	0.58	1.00	41	0.85
Mean	291.47	-293.45	0.03	794.78	2.01	8.82	0.21	0.30	9.87	0.69
Std.Dev	231.35	224.78	1.24	704.77	0.32	9.82	0.12	0.32	5.71	0.06

Weekly data obtained from the MMAR is split into two non-overlapping subsamples of equal length. This Table reports the distribution of the maxima, minima, means, variances, estimated power-law exponent,$\ddot{\alpha}$, estimated cutoffs,$\ddot{x}_{min}$, percentage of observations governed by a power law with parametrization ($\ddot{\alpha}$,$\ddot{x}_{min}$), p-values of Clauset et al.'s (2009) goodness-of-fit tests, the maximum time lengths in power-law regimes measured in terms of consecutive observations, and the estimated Hurst exponents,$\ddot{H}$for the first subsample (512 observations). Data are derived from a multiplicative cascade with binominal bending with$p = 0.80$

Table 30 Weekly multifractal return data derived from a multiplicative cascade with binominal bending and$p = 0.80$and subsample 2

Distribution	MAX	MIN	Mean	VAR	$\ddot{\alpha}$	$\ddot{x}_{min}$	% #PL state	p-value GoF	MAX #t in PL state	$\ddot{H}$
<2.5%	19.05	-237.53	-0.61	13.77	1.63	0.25	0.04	0.00	3	0.60
<5%	21.63	-199.26	-0.52	16.06	1.65	0.30	0.05	0.00	3	0.62
Median	56.58	-57.94	0.00	38.84	1.98	1.66	0.17	0.22	9	0.76
>95%	202.45	-22.02	0.50	136.31	2.55	7.34	0.42	0.92	20	0.89
>97.5%	244.38	-18.12	0.59	160.28	2.79	8.76	0.44	0.97	23	0.90
Min	10.29	-419.02	-0.94	10.51	1.53	0.11	0.02	0.00	2	0.50
Max	351.27	-11.32	1.02	364.63	3.73	12.81	0.58	1.00	44	0.99
Mean	76.92	-75.90	0.00	52.06	2.01	2.21	0.21	0.32	9.50	0.76
Std.Dev	57.51	55.82	0.31	40.25	0.30	2.20	0.12	0.32	5.38	0.08

Weekly data obtained from the MMAR is split into two non-overlapping subsamples of equal length. This Table reports the distribution of the maxima, minima, means, variances, estimated power-law exponent,$\ddot{\alpha}$, estimated cutoffs,$\ddot{x}_{min}$, percentage of observations governed by a power law with parametrization ($\ddot{\alpha}$,$\ddot{x}_{min}$), p-values of Clauset et al.'s (2009) goodness-of-fit tests, the maximum time lengths in power-law regimes measured in terms of consecutive observations, and the estimated Hurst exponents,$\ddot{H}$for the second subsample (512 observations). Data are derived from a multiplicative cascade with binominal bending with$p = 0.80$

Table 31 Weekly multifractal return data derived from a multiplicative cascade with binominal bending and$p = 0.85$and subsample 1

Distribution	MAX	MIN	Mean	VAR	$\ddot{\alpha}$	$\ddot{x}_{min}$	% #PL state	p-value GoF	MAX #t in PL state	$\ddot{H}$
<2.5%	100.00	-1916.74	-4.35	439.37	1.52	0.51	0.04	0.00	3	0.60
<5%	121.26	-1617.46	-3.65	503.60	1.53	0.56	0.05	0.00	3	0.62
Median	348.09	-346.56	-0.05	1565.57	1.78	4.10	0.19	0.15	10	0.74
>95%	1644.10	-142.63	3.96	8225.54	2.38	31.34	0.44	0.91	23	0.83
>97.5%	2017.70	-116.73	4.75	11,623.51	2.53	36.96	0.45	0.96	24	0.85
Min	52.18	-3213.14	-7.97	256.20	1.44	0.21	0.02	0.00	2	0.54
Max	3738.73	-60.32	6.58	28,036.31	2.87	60.81	0.57	1.00	37	0.90
Mean	546.55	-101.84	0.00	89.66	1.84	1.43	0.21	0.31	10.33	0.82
Std.Dev	516.01	90.26	0.41	91.41	0.26	1.78	0.12	0.32	6.03	0.08

Weekly data obtained from the MMAR is split into two non-overlapping subsamples of equal length. This Table reports the distribution of the maxima, minima, means, variances, estimated power-law exponent,$\ddot{\alpha}$, estimated cutoffs,$\ddot{x}_{min}$, percentage of observations governed by a power law with parametrization ($\ddot{\alpha}$,$\ddot{x}_{min}$), p-values of Clauset et al.'s (2009) goodness-of-fit tests, the maximum time lengths in power-law regimes measured in terms of consecutive observations, and the estimated Hurst exponents,$\ddot{H}$for the first subsample (512 observations). Data are derived from a multiplicative cascade with binominal bending with$p = 0.85$

Table 32 Weekly multifractal return data derived from a multiplicative cascade with binominal bending and$p = 0.85$and subsample 2

Distribution	MAX	MIN	Mean	VAR	$\ddot{\alpha}$	$\ddot{x}_{min}$	% #PL state	p-value GoF	MAX #t in PL state	$\ddot{H}$
<2.5%	17.28	-354.84	-0.79	13.21	1.51	0.09	0.04	0.00	3	0.65
<5%	22.90	-295.92	-0.68	16.49	1.53	0.10	0.05	0.00	3	0.67
Median	65.24	-65.96	-0.01	56.59	1.79	0.80	0.18	0.18	10	0.82
>95%	310.16	-22.73	0.68	272.79	2.38	5.60	0.43	0.91	22	0.95
>97.5%	370.90	-17.85	0.78	338.67	2.50	6.13	0.45	0.94	30	0.96
Min	7.58	-614.53	-1.27	7.14	1.44	0.03	0.02	0.00	2	0.56
Max	524.81	-8.35	1.35	759.71	3.15	13.39	0.61	1.00	44	1.02
Mean	103.02	-101.84	0.00	89.66	1.84	1.43	0.21	0.31	10.33	0.82
Std.Dev	93.09	90.26	0.41	91.41	0.26	1.78	0.12	0.32	6.03	0.08

Weekly data obtained from the MMAR is split into two non-overlapping subsamples of equal length. This Table reports the distribution of the maxima, minima, means, variances, estimated power-law exponent,$\ddot{\alpha}$, estimated cutoffs,$\ddot{x}_{min}$, percentage of observations governed by a power law with parametrization ($\ddot{\alpha}$,$\ddot{x}_{min}$), p-values of Clauset et al.'s (2009) goodness-of-fit tests, the maximum time lengths in power-law regimes measured in terms of consecutive observations, and the estimated Hurst exponents,$\ddot{H}$for the second subsample (512 observations). Data are derived from a multiplicative cascade with binominal bending with$p = 0.85$

Acknowledgements The author received useful comments from the participants of the 2024 finance research seminar at the University of Oulu. Special thanks are owed to Juha-Pekka Junttila, Petri Sahlström, and Matti Koivuranta for providing valuable comments. Furthermore, the author is thankful for having received useful comments from the participants of the 2024 finance research seminar at the University of Kiel. Special thanks are owed to Thomas Lux. The author is also grateful for having received valuable comments from the participants of the 2024 Economics & Finance Research Seminar at the University of Turin. The author is thankful to Davide Sandretto for useful comments. Finally, the author is thankful for the valuable comments provided by three anonymous reviewers.

Funding Open Access funding provided by University of Vaasa. The author received no financial support for the research, authorship, and/or publication of this article.

Declarations The author has no relevant financial or non-financial interests to disclose.

Competing interests The author reports there are no competing interests to declare.

References

Bacry, E., Kozhemyak, A., & Muzy, J.-F. (2008). Continuous cascade model for asset returns. *Journal of Economic Dynamics and Control, 32*, 156–199.

Baillie, R. T., Bollerslev, T., & Mikkelsen, H. O. (1996). Fractionally integrated generalized autoregressive conditional heteroskedasticity. *Journal of Econometrics, 74*(1), 3–30.

Bassingthwaighte, J. B., & Raymond, G. M. (1994). Evaluating rescaled range analysis for time series. *Annals of Biomedical Engineering, 22*, 432–444.

Baur, D. G., & Dimpfl, T. (2021). The volatility of Bitcoin and its role as a medium of exchange and a store of value. *Empirical Economics, 61*, 2663–2683.

Bollerslev, T., & Mikkelsen, H. O. (1996). Modeling and pricing long memory in stock market volatility. *Journal of Econometrics, 73*(1), 151–184.

Calvet, L., & Fisher, A. (2002). Multifractality in asset returns: Theory and evidence. *Review of Economics and Statistics, 84*(3), 381–406.

Calvet, L. E., & Fisher, A. J. (2004). How to forecast long-run volatility: Regime switching and the estimation of multifractal processes. *Journal of Financial Econometrics, 2*(1), 49–83.

Calvet, L. E., & Fisher, A. J. (2007). Multifrequency news and stock returns. *Journal of Financial Economics, 86*(1), 178–212.

Calvet, L., Fisher, A., & Wu, L. (2018). Staying on top of the curve: A cascade model of term structure dynamics. *Journal of Financial and Quantitative Analysis, 53*, 937–963.

Cirillo, P., & Taleb, N. N. (2020). Tail risk of contagious diseases. *Nature Physics, 16*(6), 606–613.

Clark, P. K. (1973). A subordinated stochastic process model with finite variance for speculative prices. *Econometrica, 41*(1), 135–155.

Clauset, A., Shalizi, C. R., & Newman, M. E. J. (2009). Power law distributions in empirical data. *SIAM Review, 51*, 661–703.

Fama, E. F., & French, K. R. (1992). The cross-section of expected stock returns. *Journal of Finance, 47*, 427–465.

Fama, E. F., & French, K. R. (1993). Common factors in the returns on stocks and bonds. *Journal of Financial Economics, 33*, 3–56.

Fama, E. F., & French, K. R. (2015). A five-factor asset pricing model. *Journal of Financial Economics, 116*, 1–22.

Feng, G., Giglio, S., & Xiu, D. (2020). Taming the factor zoo: A test of new factors. *Journal of Finance, 75*(3), 1327–1370.

Mandelbrot, B., Fisher, A., & Calvet, L. (1997). A multifractal model of asset returns. Cowles Foundation Discussion Paper No 1164 (pp. 1−33). Yale University.

Foley, S., Karlsen, S. J., & Putniņš, T. J. (2019). Sex, drugs, and Bitcoin: How much illegal activity is financed through cryptocurrencies? *Review of Financial Studies, 32*(5), 1798–1853.

Galbraith, J. W., & Zernov, S. (2004). Circuit breakers and the tail index of equity returns. *Journal of Financial Econometrics, 2*, 109–129.

Ghysels, E., & Jasiak, J. (1995). Stochastic volatility and time deformation: An application to trading volume and leverage effects (CIRANO Working Paper No. 95s-31). CIRANO.

Gradojevic, N., & Tsiakas, I. (2021). Volatility cascades in cryptocurrency trading. *Journal of Empirical Finance, 62*, 252–265.

Grobys, K. (2023). A multifractal model of asset (in)variances. *Journal of International Financial Markets, Institutions and Money, 85*, Article 101767.

Grobys, K. (2024). A universal exponent governing foreign exchange rate risks. *International Review of Financial Analysis, 95*, Article 103422.

Grobys, K., Han, Y., & Kolari, J. (2023). Better not forget: On the memory of S&P 500 survivor stock companies. *Journal of Risk and Financial Management, 16*(2), 126.

Hou, K., Xue, C., & Zhang, L. (2020). Replicating anomalies. *Review of Financial Studies, 33*(5), 2019–2133.

Kelly, B. (2014). The dynamic power law model. *Extremes, 17*, 557–583.

Kelly, B., & Jiang, H. (2014). Tail risk and asset prices. *Review of Financial Studies, 27*(10), 2841–2871.

Kyriazis, N., Papadamou, S., & Corbet, S. (2020). A systematic review of the bubble dynamics of cryptocurrency prices. *Research in International Business and Finance, 54*, Article 101254.

Liu, W., Liang, X., & Cui, G. (2020). Common risk factors in the returns on cryptocurrencies. *Economic Modelling, 86*, 299–305.

Liu, Y., Tsyvinski, A., & Wu, X. (2022). Common risk factors in cryptocurrency. *Journal of Finance, 77*(2), 1133–1177.

Lux, T. (1995). Herd behaviour, bubbles and crashes. *Economic Journal, 105*(431), 881–896.

Lux, T., & Alfarano, S. (2016). Financial power laws: Empirical evidence, models, and mechanisms. *Chaos, Solitons and Fractals, 88*, 3–18.

Lux, T., & Marchesi, M. (1999). Scaling and criticality in a stochastic multi-agent model of a financial market. *Nature, 397*, 498–500.

Lux, T., Morales-Arias, L., & Sattarhoff, C. (2014). A Markov-switching multifractal approach to forecasting realized volatility. *Journal of Forecasting, 33*, 532–541.

Mandelbrot, B. (2008). *The (mis)behavior of markets*. Profile Books.

Menkhoff, L., Sarno, L., Schmeling, M., & Schrimpf, A. (2012). Currency momentum strategies. *Journal of Financial Economics, 106*, 660–684.

Muzy, J.-F., & Bacry, E. (2002). Multifractal stationary random measures and multifractal random walks with log infinitely divisible scaling laws. *Physical Review, E 66*, Article 056121.

Peng, C. K., Buldyrev, S. V., Havlin, S., Simons, M., Stanley, H. E., & Goldberger, A. L. (1994). Mosaic organization of DNA nucleotides. *Physical Review. e, Statistical Physics, Plasmas, Fluids, and Related Interdisciplinary Topics, 49*(2), 1685–1689.

Quintos, C., Fan, Z., & Philips, P. C. B. (2001). Structural change tests in tail behaviour and the Asian crisis. *Review of Economic Studies, 68*, 633–663.

Russell, D., & MacKinnon, J. G. (1993). The method of maximum likelihood: Fundamental concepts and notation. *Estimation and inference in econometrics.* Oxford University Press.

Segnon, M., & Lux, T. (2013). Multifractal models in finance: Their origin, properties, and applications. Kiel Working Paper No. 1860, Kiel Institute for the World Economy.

Shen, D., Urquhart, A., & Wang, P. (2020). A three-factor pricing model for cryptocurrencies. *Finance Research Letters, 34*, 101248.

Stavroyiannis, S., Babalos, V., Bekiros, S., Lahmiri, S., & Uddin, G. S. (2019). The high frequency multifractal properties of Bitcoin. *Physica a: Statistical Mechanics and Its Applications, 520*, 62–71.

Takaishi, T. (2025). Multifractality and sample size influence on Bitcoin volatility patterns. *Finance Research Letters, 74*, Article 106683.

Wagner, N. (2003). Estimating financial risk under time-varying extremal return behavior. *Or Spectrum, 25*, 317–328.

Werner, T., & Upper, C. (2004). Time variation in the tail behavior of Bund future returns. *Journal of Futures Markets, 24*, 387–398.

White, E., Enquist, B., & Green, J. L. (2008). On estimating the exponent of power law frequency distributions. *Ecology, 89*, 905–912.